Status of the Novosibirsk High power Free Electron Laser

N. A. Vinokurov[1]

Budker Institute of Nuclear Physics,
11 Ac. Lavrentyev Prosp, 630090, Novosibirsk, Russia

Abstract : The high power infrared free electron laser is under construction in Novosibirsk. The 2-MeV injector for the accelerator-recuperator has been manufactured and tested recently. The design of the magnetic system was improved significantly to meet better the requirements of potential users. The features of the project and the current status are described.

1. Introduction

The efficiency of the conversion of the beam power to the radiation power is rather small in an FEL, being typically not more than a few percent. For high power applications, therefore, it is necessary to recover the beam power after the FEL interaction. The main reason for the energy recovery, except of simple energy saving, is the dramatic reduction of the radiation hazard at the beam dump.

One of the possible methods of the beam energy recovery is to return the beam to the radiofrequency (RF) accelerating structure, which was used to accelerate it.[1,2] If the length of path from the accelerator through the FEL to the accelerator is chosen properly, the deceleration of particles will occur instead of acceleration, and therefore the energy will return to the accelerating RF field (in other words, the beam will excite RF oscillations in the accelerating structure together with the RF generator). Such a mode of accelerator operation was demonstrated at the Stanford HEPL.[3] An obvious development of such an approach is the use of multipass recirculator[4,5] instead of simple linac. By increasing of the number of passes, cost and power consumption can be reduced. However, the threshold currents for instabilities also decrease, so the "optimal" number of passes exists.[6] The general scheme of such FEL is shown in Fig. 1.

The electron beam from the injector 1 enters the RF accelerating structure 2. After the first acceleration in

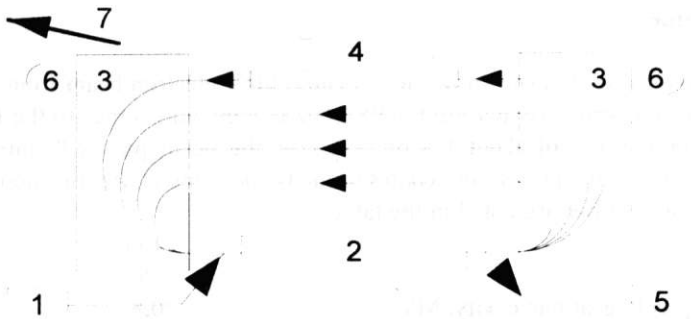

Figure 1. The scheme of the FEL with the accelerator-recuperator. 1-injector; 2-RF accelerating structure 3-180-degree bends; 4-FEL magnetic system; 5-beam dump; 6-mirrors; 7 output light beam.

[1] Corresponding author . Tel: 7-3832-394003, Fax : 7-3832-342163, e-mail : vinokurov@inp.nsk.su

the accelerating structure the beam passes through the magnetic system (bends 3 and focusing quadrupoles), which returns it to the accelerating structure for the second time. To have the acceleration of the beam at each pass though the accelerating structure it is enough to choose the orbit lengths to be integer of the RF wavelength (approximately). After several passes through the accelerating structure the beam reach the required energy and enters the FEL magnetic system 4, which is installed in the straight section of the last orbit. Here the small (about 1%) amount of the electron beam power is converted to the light. The exhaust beam returns to the accelerating structure. To provide a deceleration of the exhaust beam instead of an acceleration, the length of the last orbit is approximately half-integer of the RF wavelength. Due to the relatively small energy difference the decelerating beam follows almost the same orbits, as the accelerated one. Finally, the low-energy exhaust beam is absorbed in the beam dump 5. Some desirable features of an accelerator-recuperator are listed below.

1. The ejection (and, correspondingly, the injection) energy is to be less than 10 MeV, to avoid neutron generation in the beam dump.
2. The electron optical system has to provide proper focusing for the accelerating and the decelerating beams. It is not so trivial, as each orbit, except for the last one, is used to transport two beams (accelerating and decelerating) with the different initial conditions simultaneously, and there are many beams with very different energies inside the linac.
3. Energy acceptance is to be a few percents or larger to decelerate the spent electron beam. This can be achieved by employing magnetic system consisting of achromatic bends with low enough transverse dispersion function inside.
4. It is preferable to have a zero transverse dispersion function in the straight line sections to allow the optimization of the betatron phase advances at each orbit to increase the threshold current for the transverse beam breakup.
5. The frequency of the RF system tends to be low to decrease the longitudinal and transverse impedances and increase the longitudinal acceptance. Another advantage of low frequencies is the possibility of using the separated (uncoupled) RF resonators with individual tunes of fundamental and asymmetric modes.

To preserve low transverse emittance it is preferable to have a high peak current only at high energies. So the rotation in the longitudinal phase space by $\pi/2$, $3\pi/2$,... may be useful.

The high power infrared FEL for the Siberian center of photochemical research, which is under construction now, is the implementation of this approach.

2. Accelerator-recuperator

The accelerator - recuperator layout is shown in Fig. 2. The 2 MeV electron beam from the injector passes 8 times through the accelerating structure, getting the 98 MeV energy, and comes to the FEL, installed in the last straight section. After the loss of about 1% of its power the beam passes 8 times more through the accelerating structure, returning the power, and comes to the beam dump at the injection energy.

Some parameters of the accelerator are listed in the table:

RF wavelength, m	1.66
Number of RF cavities	16
Amplitude of accelerating voltageat one cavity, MV	0,8
Number of orbits	8
Injection energy, MeV	2
Final electron energy, MeV	98
Bunch repetition frequency, MHz	2 - 22,5
Average current, mA	4 - 50

Final electron energy dispersion, %	0,2
Final electron bunch length, ps	20 - 100
Final peak electron current, A	100 - 20

The 300 keV electron gun of the injector produces the 1 ns electron bunches with a repetition frequency up to 22.5 MHz. It has the DC power supply (rectifier) and termionic cathode with the greed. After passing the modulating RF cavity, the electron bunch is compressed in a drift section down to 200 ps and accelerated up to 2 MeV in the next two RF cavities. After that electrons are injected into the common straight section of the microtron - recuperator, using two pairs of the identical bending magnets with opposite magnetic field signs. At the entrance to the main accelerating system the bunch length is 100 ps. The project of the 300 keV photoinjector was developed [7] to replace the thermionic gun in future.

The accelerating structure consists of 16 RF cavities. Each cavity has mechanical tunings for the fundamental and high order modes. The effective accelerating voltage is 0.8 MV at the thermal power consumption about 0.1 MW. So, the total RF power is near 2 MW. The details of the RF system design and tests were described in paper.[8]

The orbit geometry was chosen to meet the following conditions:

- the lengths of all orbits (except of the eighth one) are equal to integer number of the RF wavelength;
- the distances between straight sections are equal;
- each 180 - degree bend is achromatic.

First condition is necessary for synchronous acceleration.[4] The eighth orbit is longer, than the seventh one by 1.45 of the RF wavelength to obtain deceleration at the next eight passes through the RF structure. The second make the design more compact. The third condition eliminates coupling of horizontal betatron and longitudinal motions and makes focusing more flexible. The splitting magnets are round. The quadrupoles into the 180-degree bends makes each of these bends achromatic. The quadrupoles at the long straight sections are optimized to focus properly both accelerating and decelerating beams.

The length of the straight sections was chosen such, that, when the electron bunches are injected at every eighth period of the RF voltage (e.g. with a frequency of 22.5 MHz), the bunches under acceleration and deceleration are not overlapping each other on the common track, but fill all available equilibrium phases homogeneously. In this case the interaction of the electron bunches, having various energies, decreases dramatically.

Computer simulations of the longitudinal and transverse beam dynamics show that the microtron - recuperator is capable to operate with an average current above 0.1 A. The final bunching occurs on the last track, and that allows to achieve a high peak current (about 100 A) without significant emittance degradation.

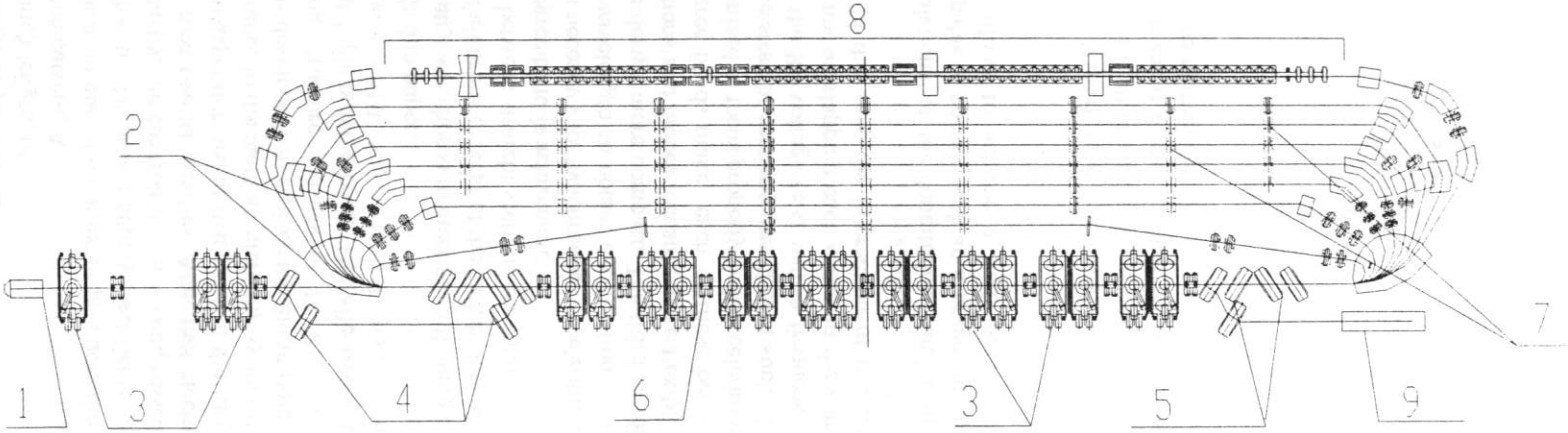

Figure 2. Scheme of the microtron-recuperator (1 - electron gun; 2 - bending magnets; 3 - RF resonators; 4,5 - injection and extraction magnets; 6 - focusing quadrupoles; 7 - straight sections with the quadrupole lenses; 8 - FEL magnetic system; 9 - beam dump).

3. The FEL

The scheme of FEL, with the electron outcoupling [9] is shown in Fig. 3. The FEL-oscillator is the optical klystron with undulators 1 and 3, dispersive section 2 and mirrors 6. The microbunched (in the FEL-oscillator and the bend 4) electron beam passes through radiator 5. As the electron beam in the radiator is deflected from the optical cavity axis, the coherent undulator radiation leaves the cavity.

As the FEL is used here only to bunch the electron beam, it has to be optimized for minimal intensity of light on the mirror surfaces. To limit the intracavity power it is convenient to choose a high value of longitudinal dispersion of the dispersive section. In addition, it is preferable to have the second undulator sufficiently longer than the first one. Then «useful» energy modulation in the second undulator, which causes the density modulation in the radiator, is significantly more than « harmful» modulation in the first undulator, which increases the effective energy spread in the radiator. To minimize this increase of the effective energy spread, the intracavity power loss must be minimized (so, mirror reflectivity has to be good).

The actual magnetic system of the FEL consists of four undulators, two bunchers (dispersive sections), and one achromatic bend. The first three undulators and two dispersive sections compose the optical klystron using as a master oscillator. The optical resonator of about 40 m length consists of two mirrors. The number of periods in each undulators is 36, length of the period is 9 cm. To simplify the wavelength tuning we use electromagnetic undulators with the maximum of deflection parameter K about 2. The reason for using of two dispersive sections is to improve the frequency selectivity. To make it clear, consider the two-undulator optical klystron. Let s is the delay of an electron, passing from the middle of the first undulator to the middle of the second one, with respect to the wavefront of light, propagating between these two points (s is also the delay between the wavetrains, emitted by an electron in undulators). The maximum amplification

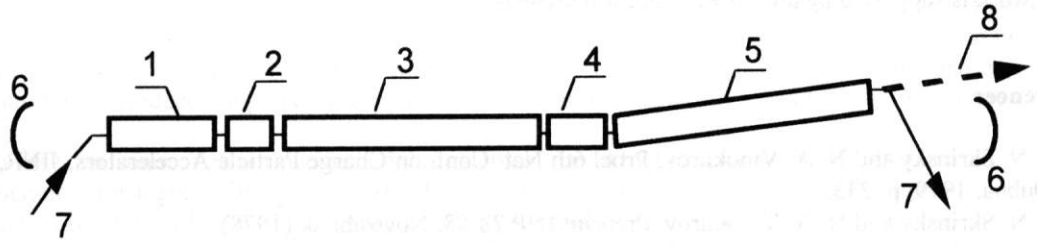

Figure 3. The scheme of the FEL. 1 – first undulator; 2 – dispersive section; 3 – second undulator; 4 – achromatic bend; 5 – undulator-radiator; 6 – mirror;7 – electron beam; 8 – coherent undulator radiation.

takes place at the wavelengths λ, which satisfy the condition $s = (n - 1/4)\lambda$, where n is the integer. If there are two bunchers and three undulators, we must satisfy two similar conditions simultaneously (for two different s_1 and s_2) to obtain the maximum. Therefore, the maxima will occur more rarely. Such a configuration offers fine and fast wavelength tuning.

The magnetic system of the achromatic bend consists of four bending magnets and focusing quadrupole lens. The detail consideration and results of tests of such achromatic bend are described in papers.[9,10] Taking into account the angular divergence of the fundamental eigenmode of the optical resonator and of the coherent radiation we chose the 4 mrad deflection angle. The distance between the center of the mirror and coherent radiation axis is 6 cm. The fourth undulator (radiator) is the same, as the previous three, but with slightly lower field amplitude (it is easy, as the undulators are electromagnetic) to maximize the output power.[11]

For the initial operation we have chosen the simplest two-mirror optical resonator. Its large length decrease the light intensity on the mirror surfaces and makes possible to obtain oscillation with a low (4 MHz) repetition frequency of the electron bunches. Therefore, we will have a low average power (and therefore, negligible heating of the mirrors), while the peak power will be high. After that we will be able to increase the average power, increasing the repetition rate of the injector pulses.

The FEL radiation will consist of pulses with 10-30 ps duration, 2-22.5 MHz repetition rate, and 2-10 micron wavelength.

4. The Current Status

The 2-MeV electron injector is in operation. The maximum average current 40 mA is achieved. The measured normalized beam emittance is 15 π mm mrad. The assembly of the RF generators and manufacturing of the RF cavities for the main accelerating structure are in progress.

Acknowledgments

This work is supported by the SB RAS grant IGSB-97-2.2.

References

[1] A. N. Skrinsky and N. A. Vinokurov, Proc. 6th Nat. Conf. on Charge Particle Accelerators, JINR, vol. 2, Dubna, 1979, p. 233.
[2] A. N. Skrinsky and N. A. Vinokurov, Preprint INP 78-88, Novosibirsk (1978).
[3] T. I. Smith et al., Nucl. Instr. and Meth. A 259 (1987) 1.
[4] R. E. Rand, Rerciculating Electron Accelerators, Harwood Academic Publishers, 1984.
[5] N. G. Gavrilov et al., IEEE J. Quantum Electron., QE-27, pp. 2626-2628, 1991.
[6] N. A. Vinokurov et al., Proc. of SPIE Vol. 2988, p. 221 (1997).
[7] N. G. Gavrilov et al., Nucl. Instr. And Meth. A 331 (1993) ABS17.
[8] V. S. Arbuzov et al., Proc. 1993 Particle Accelerator Conf. PAC 93, v.2, pp. 1226-1228.
[9] G. N. Kulipanov et al., IEEE J. Quantum Electron., QE-27, pp. 2566-2568, 1991.
[10] N. G. Gavrilov et al., IEEE J. Quantum Electron., QE-27, pp. 2569-2571, 1991.
[11] G. N. Kulipanov et al., Nucl. Instr. And Meth. A 375 (1996) 576.

Generation of Hundred Joules Pulses of 4-mm Radiation by Planar FEM with Distributed Feedbacks

N.V.Agarin, A.V. Arzhannikov[1], V.B.Bobylev, A.V.Burdakov, V.S.Burmasov, N.S.Ginzburg[a], V.G. Ivanenko, P.V.Kalinin, S.A.Kuznetsov, N.Yu.Peskov[a], S.L.Sinitsky, V.D.Stepanov, A.Yu.Zabolotsky

Budker Institute of Nuclear Physics, Novosibirsk, 630090, Russia
[a]Institute of Applied Physics, N-Novgorod, 603600, Russia

Abstract. Recent results of investigations on powerful 4-mm planar FEM with 2-D distributed feedback are described. Optimal undulator magnetic fields for effective generation were found and about one hundred joules was obtained in a pulse of 4-mm radiation for these conditions. Prospects of increasing of this value are also discussed in the paper.

1.Introduction.

One of the most promising way to increase power of FEM-generator is to use a device of planar geometry with large transverse size which is provided by planar resonator with reflectors consisting of 2-D Bragg gratings. For mode selection in such generator it was proposed to use 2-D distributed feedback [1,2].

In the first series of our experiments on the planar FEM, which were carried out at the U2-accelerator, the 1-D distributed feedback was used to obtain a narrow-band of 4-mm radiation [3]. Then, in 1998-99, these experiments were continued at the ELMI-device, based on the U-3 accelerator [4]. In this presentation we shall describe the recent series of experiments, in which 2-D Bragg gratings are used for mode selection in order to provide 2-D distributed feedback.

2. Experimental setup

2.1 Description of the ELMI-device

Because of the U-2 accelerator was strongly busied in the experiments on plasma heating studies, it was decided to transfer the research activity on the microwave generation from the U-2 accelerator to the U-3 one. For this purpose some part of experimental equipment used in experiments at the U-2 device was replaced in 1998 to the U-3 accelerator with adding a set of new elements and units. The new setup created in such way was called ELMI-device [5]. Its schematic is presented on Fig.1. The ELMI-device consists of five basic unites: a magnetically-insulated ribbon diode, a former of the sheet beam, a slit vacuum channel with undulator and resonator, a pulse magnetic system for the electron beam dumping and a diagnostic system to measure the generated radiation directly in a special vacuum chamber.

A pulse of high voltage (1MV) is applied to a strongly elongated cathode made of fibrous graphite. A graphite plate with a slit for going out of the generated beam is operated as an anode. The electron beam passes through the anode slit and then it comes with sizes 1x20 cm to a sheet beam former. The former and the undulator are located inside a slit vacuum channel with the inner cross-section 4x25cm, which has external coils producing a uniform longitudinal magnetic field up to 14 kG.

[1]Corresponding author. Tel: +7-3832-39-49-12, Fax: +7-3832-34-21-63, e-mail: arzhannikov@inp.nsk.su

The sheet beam former includes two graphite plates approaching to each other at the angle 1^0 to the central plane. These plates smoothly cut off from the beam some outer part of its cross-section so that the beam electrons have a small angular spread.

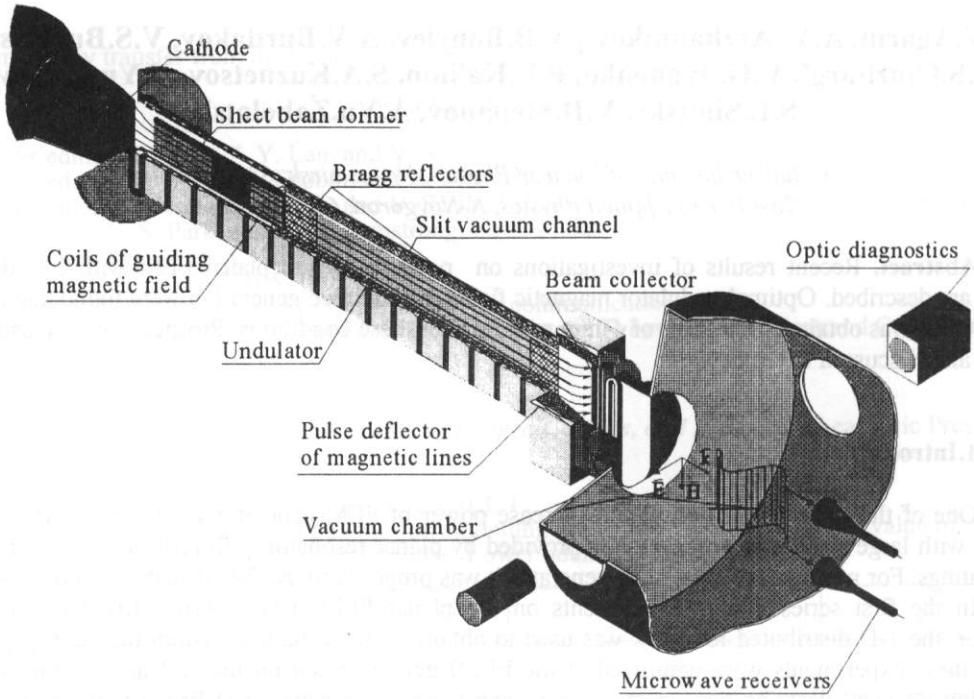

Fig.1. Schematic of the ELMI device

After passing through the former the electron beam with a cross-section 0.4x12cm comes into a planar copper resonator. The resonator consists of two Bragg reflectors connected together by a piece of a rectangular waveguide with cross-section 1x20 cm and length 64 cm. Each reflector consists of two Bragg gratings located symmetrically to the central plane. The gratings used in the first series of experiments were corrugated in one direction with a period 2mm and a depth 0.3 mm. The lengths of the reflector gratings were 18 cm and 10 cm at the entrance and at the exit of the beam from resonator respectively. In the next series of experiments, in which we studied 2-dimensional feedback, these gratings had the corrugation in two directions at the angle 45^0 to the beam axis with the period 2.82 mm and depth 0.2mm (so called 2-D gratings). In this series of research on the 2-D feedback we used the gratings with rectangular thread that was easily produced. The selective properties of these reflectors with such 2-D gratings are presented in Fig.2. The results of computer simulation in a comparison with testing experimental measurements are also shown there. The difference between experimental and theoretical data within the band 77-78 GHz we explain by the following way. Reflectivity of the 2-D Bragg reflectors within this band is connected with mode transformation from H_{01} to E_{21} but only a small part of E_{21}-mode is measured in the testing experiments. Peculiarity of this part of the frequency spectrum will be discussed in the paper [6] also presented to AFEL'99.

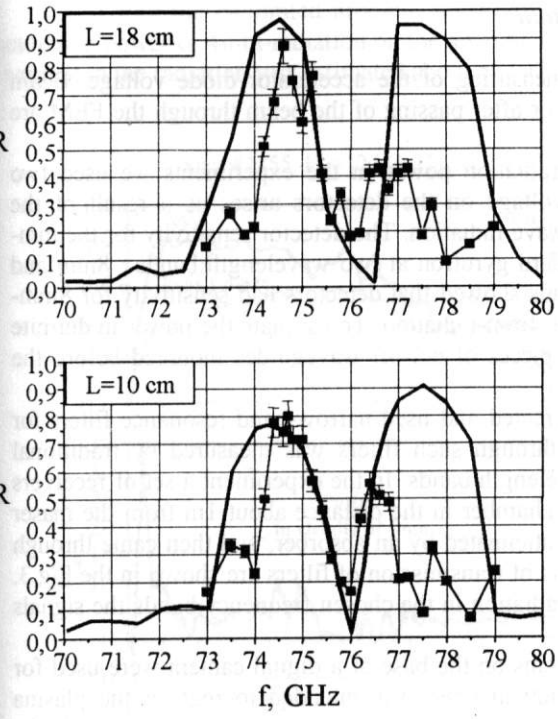

Fig.2.Selective properties of 2-D Bragg reflectors. Computer simulation – thick line, experimental measurements – square points with thin line.

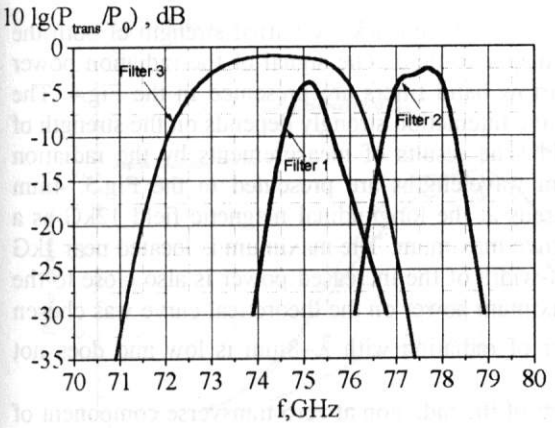

Fig.3. Filters transmission in logarithmic scale versus frequency f.

The copper plates of the Bragg resonator are embraced outside by the windings of the plane active magnetic undulator. The windings are located symmetrically on both sides of the central plane of the beam channel. Each plane winding is 96cm long and 20cm wide and contains a set of 48 multi-turn coils located one by one. The number of turns in the coil for a homogeneous part of the undulator is 15. All the coils inside a separate plate are connected consecutively but the connection polarity alternates. The cross-section profile of a separate coil was chosen so that to provide a harmonic dependence of the transverse magnetic field on the axis of the undulator. For providing adiabaticity in the pumping of the electron oscillations the number of turns in the first 6 coils is smoothly increased from 4 up to 15. To vanish amplitude of free cyclotron oscillations the current in a few entrance coils has been decreased down to 30% by their shunting by means of resistors.

The distribution of the undulator magnetic field was measured in the experiment and also obtained by numerical calculations. The spatial period was 4cm, the length of the field increase was 12cm. The maximal value of the perpendicular component of the field on the axis was 2kG when the transverse magnetic field nonhomogeneity within a resonator cross-section was less than 7% and the portion of higher harmonics on the axis was less than 1%.

In order to decline the beam electrons to the beam collector (See Fig.1) a pulse deflector of magnetic lines is used. It produces the component of the magnetic field perpendicular to the guiding field for the short time (the pulse duration is 25 μs). This system of deflector-collector should satisfy a requirement to dump the beam on a large area of the collector in order to eliminate a creation of a dense plasma near it. The plasma can absorb and reflect back the mm-radiation outgoing from the maser.

To avoid the breakdown phenomena, which can occur on the window that the microwave power went out to the atmosphere through, all measurements of the power were carried out directly in vacuum at our experiments. For such measurements a special vacuum chamber where the detectors of the millimeter radiation could be placed, was added to the exit of the vacuum channel (see Fig.1).

2.2. Diagnostics of E-beam and mm-wave radiation

Energy of the beam electrons is obtained by measuring of the accelerator diode voltage. Beam current at the entrance of the resonator and on the collector after passing of the beam through the FEM are measured by Rogowsky coils.

To measure the absolute value of microwave radiation power in the experiments we used two identical semiconductor detectors on hot electrons. A voltage on the detectors arises as a result of the resistance increase under the influence of powerful microwave radiation. The detector sensitivity for the mm-wave power of radiation was calibrated by using of standard gyrotron at two wavelength bands : 8mm and 4mm. Comparison of calibration curves for these two bands showed that detectors had sensitivity for 8mm-radiation more than 3 times larger than their sensitivity for 4mm-radiation. To estimate the power in definite ranges of the radiation wavelength we used replaceable pieces of cut-off waveguides mounted before the detector sections.

For spectral analysis of the maser radiation we created and used narrow-band resonance filters for chosen spectral intervals. The radiation power passing through such filters was measured by traditional semiconductor microwave diodes of 4mm and 8-mm wavelength bands. In the experiment a set of receivers with the filters was located inside the diagnostic vacuum chamber in the distance about 1m from the maser exit. Millimeter radiation was collected by each receiver, attenuated by an absorber, and then came through the waveguide to the resonance filter. The spectral intervals of transmission of filters are shown in the Fig.3. To obtain the average spectral density of the microwave radiation in the chosen frequency bands the signals of the diodes are divided by the bandwidth of the filters.

In addition to the microwave diagnostics the systems on the base of a digital camera were used for measuring in optical and X-ray bands. The system in optical band was intended to register the plasma appearance near the exit of the beam from the resonator. The X-ray system was intended to check the touching of the resonator's walls by the e-beam. To measure the velocity spread of the beam electrons that determines the efficiency of the beam-wave interaction a diagnostics based on scattering of the CO_2 – laser radiation on the beam, was elaborated and tested in the experiments.

3. Results of studies and discussion

In the described series of experiments with 2-D distributed feedback we varied strength of both the longitudinal and transverse components of the undulator magnetic field. The signal of the radiation power detector together with signals of the MW-diodes with narrow band filters are presented in the Fig.4. The experiments have shown that the efficiency of the beam–wave interaction strongly depends on the strength of the transverse component of the undulator magnetic field. The results of measurements by the radiation power detectors in two wide bands near 4mm and 8mm wavelengths are presented in the Fig.5. 4mm radiation power measured by the detectors with hot electrons at the longitudinal magnetic field 12kG as a function of the transverse undulator field has a very distinctive maximum. The maximum is located near 1kG as it has been predicted by theoretic calculations. The half-width of the increased power is also close to the value predicted by theory. It should be pointed that the maximum power on the theoretical curve was chosen as equal to the experimental one. In own turn, the power of radiation with λ~8mm is low and does not exceed 20% of total power.

Other important experimental fact is that the power of the radiation at zero transverse component of the undulator field is negligibly small. It points to the absence of the mm-wave generation on the cyclotron motion of the beam electrons at these experiments. Agreement between experimental and theoretical data at the value 10kG of the longitudinal magnetic field is somewhat worse that points to influence of the cyclotron electron motion.

Using the calibrated absolute sensitivity of the radiation power detectors we measured maximal radiation power of 4mm-radiation on the level of 100MW, that is about 5% of the beam power. Total energy content in the radiation was estimated about of 100J for these conditions.

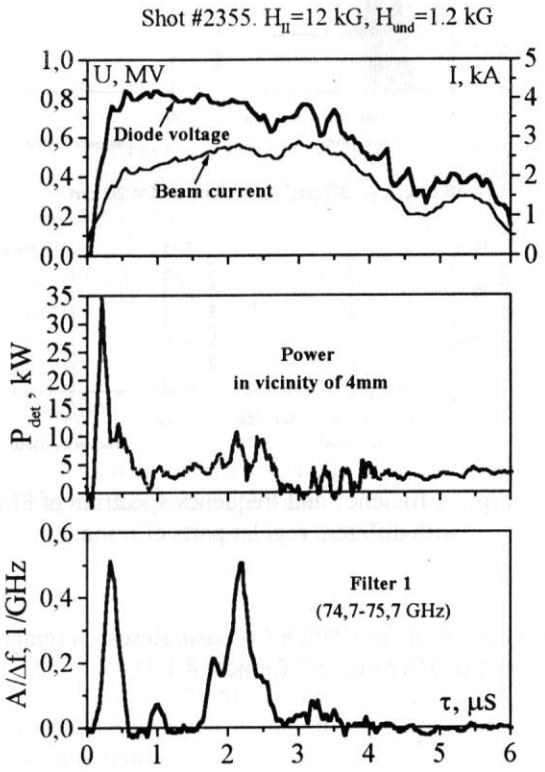

Fig.4. Generated power of 4-mm radiation

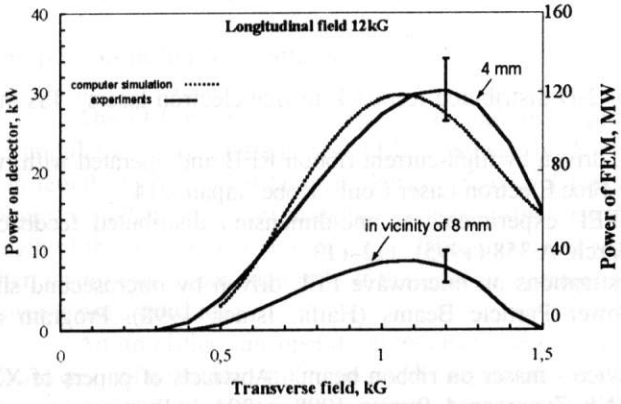

Fig.5. Power as a function of transverse field

Spectrum structure of the maser radiation in the vicinity of the operating frequency 75GHz was analysed in the experiment by means narrow-band filters. The signals from the diodes placed after the filters were divided by the width of the filter's bands. The signals modified in such way are presented in the Fig.6 for 10 kG of longitudinal field. From the relation of the average spectral density of radiation in three frequency bands one can make the following conclusion. The highest spectral density of generated radiation is located in the range 74-76GHz that corresponds to the frequency band of the resonator eigen modes. About 20% of that quantity is registered in the range 76-80GHz that is occurred due to the mode conversion of TEM H_{10} mode to the highest modes on the corrugation of the grating. The spectral density of the radiation with frequency less than 74GHz, according to the measurements, is too small.

Computer simulation of 4mm-wave generation by the FEM with the parameters of our experiments gave the electron efficiency on the level about of 7% that was close enough to experimentally obtained one (See Fig.7a). In the picture of efficiency time behavior one can see a very large noise connected with competition of the resonator modes. This result was obtained for length of regular part of resonator L_0=64cm (the distance between the reflectors). The computer simulation for other values of this distance showed that the optimal value of this parameter should be 32cm. Efficiency of the FEM as a function of time for L_0=32cm is presented in Fig.7b. One can see that the electron efficiency reaches 17% and the frequency spectrum contains only one mode. Basing on these results we have prepared new series of experiments with this distance between reflectors in the resonator.

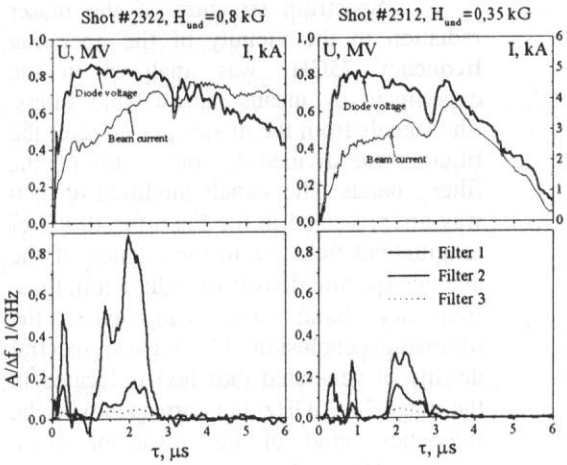

Fig.6. Spectral properties of generated radiation

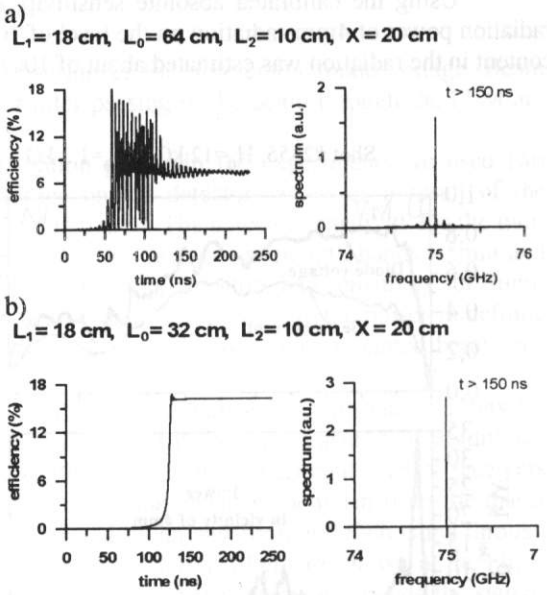

Fig.7. Efficiency and frequency spectrum of FEM with different regular parts of resonator.

Work is partially supported by ISTC (grant #531), Russian Foundation for Basic Research (grant # 97-02-7379), and Russian Interdisciplinary Program "Physics of Microwaves" (project # 1.3).

Acknowledgements

We are grateful to Prof. V.S.Koidan for his support of the work and Dr. V.S.Nikolaev and A.F. Rovenskikh for help in preparation of experiments.

References

[1] N.S.Ginsburg et al. 1992, "Using of 2-D distributed feedback in free electron lasers". Pis'ma v ZhTF, vol.18, no.9, 23-28 (in Russian).

[2] A.V.Arzhannikov et al. 1992, "FEL driven by high-current ribbon REB and operated with two-dimensional feedback", Tech. Digest of 14th Int. Free Electron Laser Conf., Kobe, Japan, 214.

[3] A.V.Arzhannikov et al. "Ribbon-FEL experiments at one-dimension distributed feedback". Nuclear Instruments & Methods in Physics Research, A 358 (1995), 112-113.

[4] N.V.Agarin et al. Progress in investigations on microwave FEL driven by microsecond sheet beam». 12-th International Conf. On High-Power Particle Beams (Haifa, Israel, 1998), Program and Abstracts, p. 262.

[5] A.V.Arzhannikov et al. "ELMI-device - maser on ribbon beam". Abstracts of papers of XXV Zvenigorod conference on plasma physics and CNF, Zvenigorod, Russia, 1998, p. 204. In Russian.

[6] An Yen Huan et al. "Selective Properties of Planar Resonators with 1-D and 2-D Feedbacks for Microwave FEM". AFEL'99, Advanced Program, p. 12.

A project of high-power CW mm-wave FEL

Sergey V.Miginsky[1]

Budker Institute of Nuclear Physics, Novosibirsk, Russia

Abstract : A project of mm-wave free electron laser driven by a 2 MeV CW high-power electron injector is described. The FEL consists of a waveguide placed inside a short-period (~10 mm) undulator. The injector provides 2 nC, 2 MeV (full energy) electron bunches of subnanosecond duration at repetition rate up to 22.5 MHz. The FEL can operate as both an amplifier or an oscillator. Supposed wavelength ~ 1 mm, average power ~ 3 kW, that can be increased up to ~ 25 kW if the repetition rate is raised to 180 MHz. Estimations of various significant parameters of the FEL and schematic design are presented.

Introduction

As it is clear from [1], an electron injector for the Novosibirsk high power FEL is ready now. Its most significant parameters are

Kinetic energy of electrons	up to	1.5 Mev,
Charge of bunch	up to	2 nC,
Bunch duration		50...500 ps,
Repetition rate	up to	22.5 MHz,
Average beam current	up to	45 mA,
Average beam power	up to	70 kW.

A reasonable question is how to use this beam now as designing and assembling of the mentioned FEL takes some time.

The very rough estimation is that. If one takes an undulator of period $\Lambda \sim 1$ cm, he obtains emission of wavelength $\lambda \sim \Lambda / (2\gamma^2) \sim 0.3$ mm. Taking electron efficiency ~5% one can expect average output power ~ 3 kW.

One-pass amplifier or oscillator?

The FEL proposed can operate as both an amplifier or an oscillator. Consider these possibilities. An undulator in an oscillator should be comparably short (main advantage), probably not longer than the gain length. On the other hand it claims a resonator (open one or a cavity), that seems to be complicated enough. Another important drawback is that in this case the minimum repetition rate is determined by the length of the resonator. Even for 22.5 MHz (maximum repetition rate of the injector) its length is ~ 6.7 m. Then lasing can be obtained only if the injector operates at full power. Adjustment of the machine at high power is not a good idea.

An amplifier can operate at arbitrary repetition rate so permits adjustment at low power (main advantage). Its undulator should be much longer, but, as showed below, not dramatically long. It claims also an oscillator of appropriate power to get coherent radiation, but these oscillator may be comparably weak.

[1] Tel: +7-3832-394443, Fax : +7-3832-342163, e-mail : S.V.Miginsky@inp.nsk.su

There are many other advantages and drawbacks of the schemes, but not so significant. In total, an amplifier seems to be better choice. Only this possibility is considered further.

A waveguide and an undulator

Lets consider a H_{11} mode [2] of angular frequency ω in a round waveguide of radius r. If one places this waveguide in a planar undulator of period Λ and deflection parameter K, then the condition of synchronism between the wave and the electrons is

$$k\left(1+\frac{1+K^2/2}{2\gamma^2}\right)-k_z=\frac{2\pi}{\Lambda}.$$

As usual in a waveguide FEL, there are two synchronous wavelengths for one set of parameters. Of course, the smallest one is using for lasing. If one take not a round waveguide, the dependencies look the same, but some "efficient" radius of the waveguide should be taken.

Let's estimate the effective cross-section of wave in the waveguide. Power of the wave is

$$P=\frac{1}{2}\int \vec{E}\times\vec{H}\,d\vec{S}=\int_0^r r\,dr\int_0^{2\pi}d\varphi\left(E_r H_\varphi-E_\varphi H_r\right)=$$

$$=\frac{Z_0}{2}\left(\frac{\lambda_c}{\lambda}\right)^2\sqrt{1-\left(\lambda/\lambda_c\right)^2}\,\frac{\pi}{k_r^2}\left[\frac{p_{11}'^{\,2}}{2}J_0^2(p_{11}')+\left(\frac{p_{11}'^{\,2}}{2}-1\right)J_1^2(p_{11}')\right],$$

where Z_0 is impedance of vacuum, λ wavelength in free space, λ_c critical wavelength of the waveguide mode, k_r radial wavenumber, J_i Bessel functions, $p'_{11}\cong 1.841$ first root of derivative of first Bessel function. Then the effective cross-section of the mode is

$$\xi=\frac{P}{|E^2|}\cong 0.2387\sqrt{1-\left(\lambda/\lambda_c\right)^2}\,\frac{\pi r^2}{Z_0}\ [\mathrm{m}^2\cdot\Omega^{-1}].$$

Gain length

One needs comparably high amplification to get saturation power level from weak master oscillation. In this case amplification increases approximately exponentially with the undulator length. The equation system analogous to one of travelling-wave tube (see [3] and references there) describes behavior of electric field E in the waveguide, and deviations of relativistic factor $\delta\gamma$ and longitudinal coordinate δz of electrons from the average values. There are three solutions having dependency $\exp \kappa z$. The only increasing solution is

$$\mathrm{Re}\,\kappa=\frac{\sqrt{3}}{4\gamma}\sqrt[3]{\frac{K^2}{2\gamma}\frac{eI}{m_e c^2\tilde{\beta}\gamma}\left(1+K^2/2\right)\frac{2\pi}{\lambda\xi}}=\frac{\sqrt{3}}{4\gamma}\sqrt[3]{\frac{K^2}{\tilde{\beta}}\frac{eI}{m_e c^2}\frac{2\pi}{\Lambda\xi}}$$

Restrictions

Due to strong vertical focusing in a planar undulator the equilibrium Twiss β-function inside it is small enough.

$$\beta = \sqrt{2}\rho = \sqrt{2}\,\frac{\Lambda\gamma\sqrt{1-1/\gamma^2}}{2\pi K}.$$

It leads to significant angular spread of electron beam of finite emittance and hence to spread of longitudinal velocities of electrons. The effect of angular spread can be neglected if

$$\frac{(\Delta\vartheta)^2}{4} = \frac{\varepsilon}{4\beta} \le \frac{\lambda}{2\pi L} \Rightarrow \varepsilon \le \frac{\lambda \cdot 4\sqrt{2}\Lambda\gamma\sqrt{1-1/\gamma^2}}{2\pi L \cdot 2\pi K} \approx 90 \text{ mm·mrad},$$

where gain length $L \approx 30$ mm, $\gamma = 4$, $K = 1$, $\Lambda = 10$ mm were taken.

Then, the beam should pass through the waveguide with no sufficient loss. Thus another restriction for vertical emittance is

$$\sqrt{\beta\varepsilon} \le r/3 \Rightarrow \varepsilon \le \frac{\sqrt{2}\pi K r^2}{9\Lambda\gamma\sqrt{1-1/\gamma^2}} \approx 30 \text{ mm·mrad},$$

where the same values and $r = 1.5$ mm are taken.

Energy spread of the beam causes spread of longitudinal velocities of electrons due to dispersion in the undulator. The effect is not dramatic if

$$\frac{\Delta p}{p} \le \frac{\Lambda}{5L} \approx 0.04 \rightarrow \Delta p \le 80 \text{ keV}.$$

Then one can estimate maximum pulse duration as the accelerating field produces energy spread due to its cosine form

$$\Delta t \le 2\frac{\sqrt{2\,\Delta p/p}}{2\pi f} \approx 0.5 \text{ ns}.$$

Spontaneous emission

Consider only H_{11} modes inside the amplification band of the FEL. Power lost by the beam to a single mode

$$P_{sp} = \frac{K^2}{16\gamma^2}\frac{v_{gr}}{\xi} IeL.$$

If one takes a cavity of amplification length, there are $N \approx \Lambda/\lambda_w$ resonance modes in the amplification band, and NP_{sp} is an estimated value of the input noise of the FEL amplifier.

Space charge effect

Due to bunching in the FEL variation of space charge density along the axis of the beam is $\kappa_0 \sin kz$, then the longitudinal electric field produced by this space charge wave in the particle rest frame is

$$E = \frac{\kappa_0}{2\pi\rho^2\varepsilon_0} \cdot 2\int_0^\infty \left(1 - \frac{z}{\sqrt{z^2+\rho^2}}\right) \sin kz \exp -\xi z \, dz \cong \frac{\kappa_0}{2\pi\varepsilon_0}\left[-\frac{k}{2}\ln\frac{\left(\xi^2+k^2\right)\rho^2}{4} - (2\gamma_0 - 1)/2\right]$$

where ρ is radius of beam, $\xi \cong 2.4/r$ shielding decrement. This field should be added to the equation for amplification length. In the laboratory frame each k is substituted by k/γ. One can estimate this effect is negligible in the considered FEL.

Losses in the waveguide

Damping

$$D = \frac{2\pi\ rS}{P} \cong \frac{8}{.319r}\sqrt{\frac{\pi\ \rho}{\lambda\ Z_0}}\ \frac{J_1^2(p'_{11})}{p'^2_{11}}\ \frac{1+\left(p'^2_{11}-1\right)\left(\lambda/\lambda_c\right)^2}{\sqrt{1-\left(\lambda/\lambda_c\right)^2}}.$$

Let $\rho = 1.8\cdot10^{-8}$ Ω·m (copper) and $r = 1.5$ mm, and obtain damping ≈ 0.8 m^{-1} for any reasonable parameters. One can see damping is much less than amplification, so it can't affect FEL operation, but lost power can overheat waveguide walls. Assume maximum power density to the walls $S_{\max} = 10^6$ W·m^{-2} (water cooled) and obtain average power limit for the FEL

$$P \le \frac{S_{\max} 2\pi r}{D} \approx 1.2\cdot10^4 \text{ W}.$$

Proposed design

Three possibilities were considered: (1) a helical undulator with a round waveguide, (2) an elliptical undulator with a rectangular waveguide, and (3) a planar undulator with a rectangular waveguide. All schemes possess advantages and drawbacks, the last one seems to be best choice, so only its parameters are discussed below.

Let's choose a planar undulator of 12.5 mm period, $K = 0.5$, and horizontal focusing ~ 0.7 T/m made by a Panovsky lens. Put a rectangular, elliptical, or "special-shaped low-loss" waveguide of vertical size 3 mm and "effective" horizontal one 6 mm inside it. Take the "effective radius" 2 mm for estimation of wavelength, gain, spontaneous emission, etc.

Dependence of wavelength on γ ("electronic tuning") is placed below.

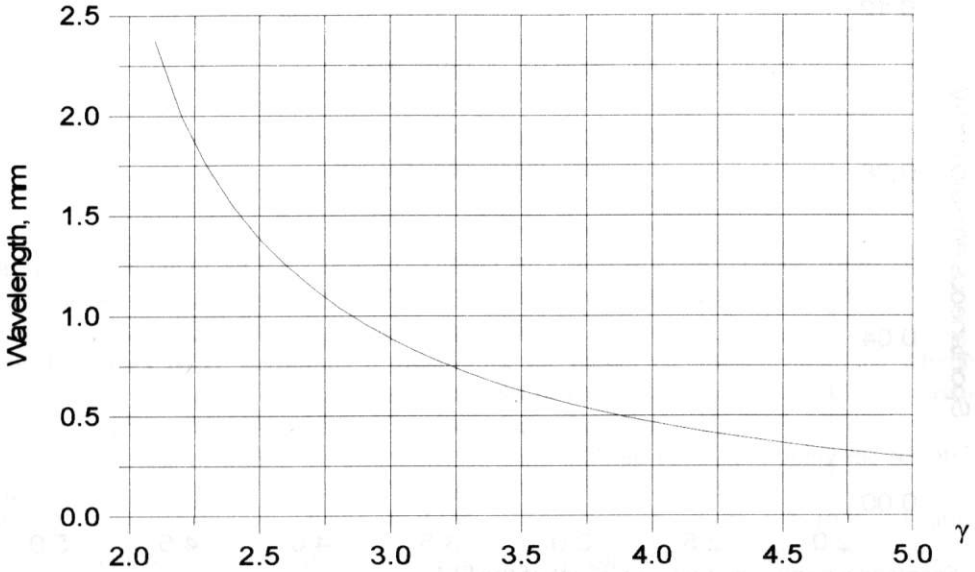

Figure 1. Wavelength emitted vs relativistic factor of the beam.

Varying γ between 2.5 and 4, one covers band 0.5...1.5 mm.

Vertical emittance should be less than ≈11 mm·mrad to conduct the beam through the waveguide. Restriction for horizontal one is much weaker.

Taking into account space charge effect, one obtains the following values of amplification lengths.

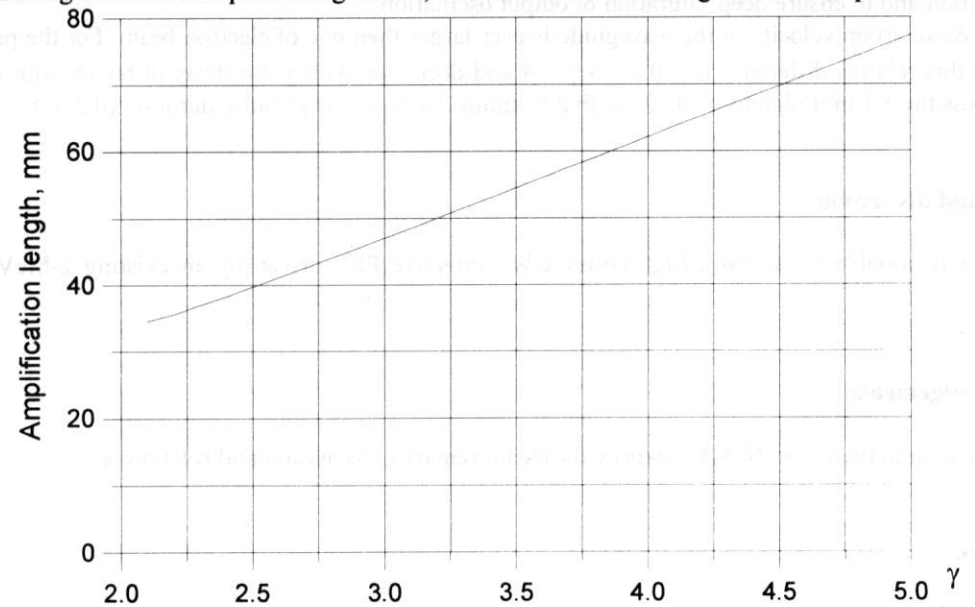

Figure 2. Amplification length vs relativistic factor. $I = 10$ A, $K = 0.5$, $r = 2$ mm and $\Lambda = 12.5$ mm.

One can see amplification length is approximately proportional to γ and ranges from 3 to 4 undulator periods.

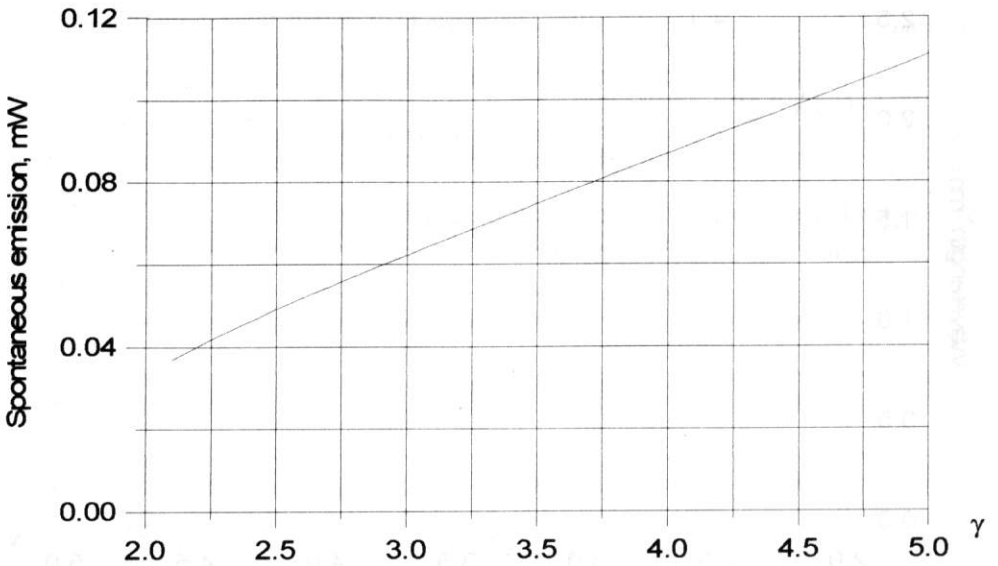

Figure 3. Spontaneous emission (not amplified) of the FEL.

As spontaneous emission, that is noise at the input of the FEL, doesn't exceed 100 μW, an ordinary CW or pulsed backward wave tube of output power several or hundred mW can be used as a master-oscillator. Taking input power 100 mW and saturation pulse power 700 kW (10 A, 5% efficiency), obtain necessary length of the undulator 1.1 m. It should be longer due to energy spread of the beam decreasing amplification and to ensure deep saturation of output oscillation.

Wave group velocity in the waveguide is ever larger then one of electron beam. For the parameters proposed this relative difference is ≈ 0.03 at $\gamma = 4$ and decreases with γ. So delay of bunch with respect to wave across the 1.1 m undulator is 0.12 ns, that is almost twice less than pulse duration (0.2 ns).

Results and discussion

It is possible to design a high-power CW mm-wave FEL driven by an existing 2-MeV electron injector.

Acknowledgements

I wish to thank Dr. N.A.Vinokurov for useful remarks, discussion and references.

References

[1] N. A. Vinokurov, Status of the Novosibirsk high power FEL, this Proceedings
[2] J.A.Stratton. Electromagnetic theory. N.Y.-L., MsGraw-Hill, 1941.
[3] T.C.Marshall. Free-Electron Lasers, New York, 1985.

Compact Far-Infrared Free-Electron Laser Driven by a Microtron

Young Uk Jeong, Byung Cheol Lee, Sung Oh Cho, Sun Kook Kim, and Jongmin Lee

Lab. for Quantum Optics, Korea Atomic Energy Research Institute, P. O. Box 105, Yusong, Taejon, 305-600, Korea

Grigory Kazakevich, Pavel Vobly, and Vitaliy Kubarev

Budker Institute of Nuclear Physics, Lavrentyev ave., 11, 630090 Novosibirsk, Russia

Abstract : We have developed a compact far-infrared FEL on the base of 8 MeV, 50 mA microtron. The wavelength of the FEL is from 100 to 200 μm depending on the magnetic strength of U-25 undulator from 5 – 6.5 kG. The period of the undulator is 25 mm and the total length is 2 m. The undulator has extremely low field error of 0.05% from the peak amplitude. We installed the horizontal focusing field of 20 G/cm inside the undulator, which provides a single period betatron motion of electrons in horizontal plane. The vertical motion of the electrons in the undulator is mainly determined by the gradient filed of the undulator. The effective number of the betatron periods in vertical plane is approximately 7 through the 2-m undulator. The resonator of the FEL is composed by a confocal scheme in horizontal plane with cylindrical mirrors and a parallel-plate waveguide with the gap of 2 mm in the vertical plane to increase the coupling between electron beam and radiation. We have observed the coherent effect of the spontaneous emission with the power enhancement more than 100 times. We will report the preliminary results of the FEL including the startup process of lasing depending on the cavity length detuning.

1. Introduction

Free electron laser (FEL) is one of the most useful light source in the wavelength region of far infrared (FIR) with its wide tunability and high peak power [1 – 4]. Recently, there are several trials to develop compact laboratory scale FELs in the FIR region with low cost [5 – 8]. The compactness and beam quality of electron beam source with energy of several MeV are crucial factors for the FELs. In small scale radio frequency (RF) accelerators, main part of its cost depends on RF system.

Conventional microtron driven by RF source of magnetron is a compact electron beam source with its

volume of 2 or 3 m^3 including pulse modulator and RF generator. It can provide high quality electron beam of low emittance and energy spread. Magnetron can generate RF power of several MW without additional amplifier. It is much cheaper than klystron based RF system. However, stability of the RF spectrum from the magnetron should satisfy the required conditions for FEL oscillation.

We have developed a compact FIR FEL on the base of an 8 MeV microtron driven by a magnetron. The microtron can provide 50 mA electron beam with pulse duration of 5 μs and the volume of the microtron system is only 2 m^3 including a pulse modulator and the RF system. The RF system has been developed to provide frequency stabilized RF power for the FEL operation. The shot to shot frequency stability of the RF power is better than 10^{-5}. The intrapulse stability of the 5 μs RF spectrum was investigated to estimate the effect to the FEL gain reduction[9 - 10]. The wavelength of the radiation is designed to be 100 – 200 μm with a high precision tunable electromagnetic planar undulator. The period of the undulator is 25 mm and the number of the undulator period is 80. The magnetic field strength can be tuned from 5 to 6.5 kG with its extremely low r.m.s error of 0.05%[11]. The resonator of the FEL is composed by a confocal scheme in the horizontal plane with cylindrical mirrors and a parallel-plate waveguide with the gap of 2 mm in the vertical plane to increase the coupling between electron beam and radiation. We have observed the coherent effect of the spontaneous emission with the power enhancement more than 100 times. We will report the preliminary results of the FEL including the startup process of lasing depending on the cavity length detuning.

2. Design issues and system configuration

There have been several trials to develop FIR FEL with microtron as a beam source. Most of them were not successful due to its low gain mainly by the low current of the electron beam, low coupling ratio between electron beam and radiation mode in the resonator, and the additional reduction of the gain by beam instabilities. Main issues to design the microtron driven FIR FEL are to maximize the FEL gain and to minimize the gain reduction factors including the resonator losses. The issues concern high performance undulator, high coupling and low loss resonator, and investigation on the effect of electron beam instabilities to the FEL gain.

To get the maximum gain, we have focused to develop a strong and high precision electromagnet undulator with the optimized length[11]. The length of the undulator should be determined by the energy spread of the electron beam and it can be evaluated by the following relation,

$$N_{max} = (4\delta E/E)^{-1}$$

where N_{max} is the number of the undulator periods for maximum gain and $\delta E/E$ is the energy spread of the electron beam. The total length of the undulator is 2 m with 25 mm period by 80. The configuration of the undulator is same as that of the 30 μm FIR FEL undulator[12], which uses permanent magnets to reduce the saturation in the iron poles. The undulator can provide strong magnetic field with low field error. The measured magnetic field strength on driving current from the U25 undulator is shown in Fig. 1. The a extremely low field error. The magnetic field strength can be tuned from 5 to 6.5 kG with the current on main coils. We have improved the accuracy of the undulator with modular pole structure. The structure makes its fabrication and assembling much easy and the cost and time for the undulator also reduced significantly. Without any correction of the undulator field, we got incredibly low r.m.s field error of 0.1%. For further improving the accuracy, we have used finite turn-number correctors from 1 to 7 turns. After measuring the field distribution, we can determine the values for correction and it can be coincide to the turn numbers of the correctors in the poles. The correctors were connected serially and one power supply is enough for driving all correctors. As a result, we can get extremely low field error of 0.05%, which is close to the accuracy of the measurement system.

The resonator of the FEL is composed by a confocal scheme in the horizontal plane with cylindrical mirrors and a parallel-plate waveguide with the gap of 2 mm in the vertical plane to increase the coupling between electron beam and radiation mode. The waveguide is fabricated by aluminum to keep higher reflection coeffiecient for FIR and non magnetic properties to the undulator field. It contains the gates for two OTR screens and the electron beam. The waveguide is aligned to be less than 0.1 mm height fluctuation through 2780 mm. The 2 mm gap of the waveguide is determined for the transport of the electron beam. The diameter of the electron beam envelope in vertical plane of the undulator is less than 1 mm and all electrons can be transported through the waveguide of 2-mm gap and 2780-mm length.

Some of the groups had used the higher power RF system with the klystron to increase the beam current and RF frequency stability. However, the trials were not successful. The problem is connected with the RF instability caused by the periodic interaction of the electron beam and RF in a accelerating cavity[9 - 10]. The instability of the RF makes timing fluctuation of the electron beam micropulses and it prevents the exact overlapping between round tripped radiation and successively injected electron beams at the resonator. The higher current with the higher RF power at the cavity increases the fluctuation amplitudes of the RF instability and it reduces the FEL gain. Therefore, the effect of the RF instability should be considered for the design of the microtron driven FEL.

The center frequency of the magnetron is determined by the resonance frequency of the accelerating cavity with the feedback locking effect. For the operation, we have used an extremely short RF line between

the magnetron and the accelerating cavity and the loss of a ferrite insulator for the reflected wave is less than 15 dB. The measured spectrum of the RF power shows Fourier limited bandwidth of the 5 μs pulse. The shot to shot stability of the RF frequency is less than 10^{-5} and the value is quite enough for the FEL oscillation with a fixed cavity length. We have measured the intrapulse instability of the electron beam micropulses by using the heterodyne method between a reference RF signal and the excited wakefield by a straight-flight monitoring cavity with the electron beam[9 - 10]. The effect of the instabilities to the FEL oscillation is investigated and the detail contents are described in the reference 12.

Schematic layout of the main system is shown in Fig. 2. In control room separated by 50 cm concrete wall from the system, there are a PC for operation and 4 racks for electric units including power supplies, CAMAC, and diagnostic devices. The whole FEL system can be installed in usual small scale laboratories. Main parameters of the system is listed in Table 1. The energy of the electron beam is 6 - 8 MeV depends on the magnetic strength of the microtron main magnet. The macropulse duration of the electron beam is 5 μs with the pulse current of 50 mA. Electrons accelerated by the microtron is transported through the beam line with 3 bending magnets and 6 quadrupoles. We can control the input condition of electron beam to the undulator for optimum laser operation. The beam line also includes electron beam diagnostics of a current transformer and an optical transition radiation (OTR) screen. The OTR screen with the beam optics has been used for measuring Twiss parameters of the electron beam.

3. Coherent spontaneous emission

We have measure the spontaneous emission without resonator mirrors. A liquid Helium cooled Ge:Ga detector has been used to measure the power and the temporal evolution of the FIR radiation[13]. The detector including a FIR window was calibrated at the wavelength of 120 μm with a stable water vapor laser. The detector is shielded from the high energy radiation and the electromagnetic noises with lead bricks. From the measurements, the minimum detectable power with the detector is less than μW. A crystal quartz lens is used to focus the emitted radiation to the detector and the capturing ratio of the detector from the total radiation power is approximately 20%.

Figure 3 is the typical evolution of the spontaneous emission. Inside the figure, the temporal shape of the electron beam is shown for comparison with the radiation. Generally, the temporal shape of the spontaneous emission follows that of the electron beam. However, we can see the spiking pulses of the radiation power at the figure, which means nonlinear process of the radiation to the electron current. The total power of the undulator radiation is calculated to be less than 1 mW in the case of incoherent radiation.

However, measured power is more than 100 mW. The measured power of the radiation is more than 100 times stronger than the calculated value of the incoherent radiation power. The enhancement of the radiation power can be explained by the effect of coherent radiation.

There have been observations on the coherent radiation with the electron beam whose bunch length is comparable to or less than the radiation wavelength[14 - 15]. Recently, there have been reports on the coherent radiation with electron beam much longer than the radiation wavelength[6, 16]. With the typical shape of the electron beam, power enhancement of 10^3 times was measured with the electron beam whose bunch length is 30 times longer than the wavelength of the radiation. The total radiation power from the electron beam in a periodic magnetic structure can be expressed to be

$$P_t = NP + N^2PF$$

where N is the number of electrons in the bunch, P is the radiation power by single electron, and F is the form factor of the electron distribution.

Figure 4 shows the dependence of the radiation power on the current of the electron beam. We can see the quadratic dependence of the radiation power on the beam current. It shows another evidence of the coherent effect in the spontaneous emission.

4. Start up of lasing

FEL oscillation experiment has been performed with the cylindrical mirrors coated by gold. Outcoupling mirror has a hole with the diameter of 0.7 mm. The coupling ratio is approximately 1% from the intracavity power. The alignment of the resonator mirror is done by using collimated beams from two HeNe lasers. The alignment accuracy and stability of the mirrors are less than 0.05 mrad. The electron beam is also aligned to the axis of the optical resonator with two OTR screens located both ends of the undulator. The positioning accuracy and stability of the electron beam is 0.1 mm. The accuracies satisfy the requirement of the confocal and waveguide mode resonator.

Power of the outcoupling radiation from the FEL oscillator was measured by changing the length of the resonator, which is shown in Fig. 5. We can see the power dependence on the cavity tuning, which means lasing process. The power increases with the detuning of cavity length from the resonance condition. The temporal evolution of the radiation power with the cavity length of -1.6 mm less than that of resonance condition is shown in Fig. 6, and it is compared with that of longer cavity length. We can see significant

enhancement of the pulses. The results shows the FEL oscillator is in the startup process of lasing. However, the lasing process is not enough to get the saturation level.

Now, upgrade of the resonator is under process to reduce the diffraction loss. We hope to see the saturated laser power with a new resonator having total loss less than 6% including outcoupling ratio.

5. Conclusion

We have developed the 100 μm range FIR FEL with the compact electron beam source of microtron. The main issues for designing the microtron based FEL have been investigated to get the optimized values for the FEL gain. The measured spontaneous emission shows 100 times higher power than the calculated value of the incoherent radiation. The effect can be explained by the coherent effect with the typical shape of the short electron beam bunch length. We have measured the quadratic dependence of the radiation power on the electron beam current and it provides a additional evidence of the coherent radiation. The FEL oscillation has been investigated by duning the cavity length and we have measured the start up process of the FEL lasing. We hope to get saturated power of the FIR FEL by reducing the diffraction loss of the optical resonator.

References

[1] D. Dlott and M. Fayer, IEEE J Quantum Electro. QE-27 (1991) 2697.

[2] R. J. Bakker, *et al.*, Phys. Rev. E 48 (1993) R3256.

[3] R. Kato, *et al.*, Nucl. Instr. and Meth., A 407 (1998) 157.

[4] Jongmin Lee, *et al.*, Nucl. Instr. and Meth., A 407 (1998) 161.

[5] R. Akberdin, *et al.*, Nucl. Instr. and Meth., A 405 (1998) 195.

[6] J. Schmerge, *et al.*, IEEE J Quantum Electro. QE-31 (1995) 1166.

[7] P. W. van Amersfoort, *et al.*, Nucl. Instr. and Meth., A 296 (1990) 217.

[8] G. Ramian, Nucl. Instr. and Meth., A 318 (1992) 225.

[9] G. Kazakevich, *et al.*, "Measurements of Intrapulse Instabilities in the Electron Beam of high Current Electron Beam", 4th Asian Symposium on FELs, Taejon, Korea, 1999.

[10] G. Kazakevich, *et al.*, "The Straight-Flight Cavity for Monitoring of Microtron Intrapulse Instabilities", 4th Asian Symposium on FELs, Taejon, Korea, 1999.

[11] Y. U. Jeong, *et al.*, "U-25 Undulator for KAERI FIR FEL", 4th Asian Symposium on FELs, Taejon, Korea, 1999.

[12] S. K. Kim, *et al.*, 4th Asian Symposium on FELs, Taejon, Korea, 1999.

[13] V. Kubarev, *et al.*, 4th Asian Symposium on FELs, Taejon, Korea, 1999.

[14] Y. U. Jeong, *et al.*, Phys. Rev. Lett. 68 (1992) 1140.

[15] Y. U. Jeong, *et al.*, Phys. Rev. E 47 (1993) 1313.

[16] D. Jaroszynski, *et al.*, Phys. Rev. Lett. 71 (1993) 3798.

Table 1

Main parameters of the KAERI FIR FEL

Electron Beam	
Electron Beam Energy	6 - 8 MeV
Macropulse Current	40 mA
Horizontal Emittance	3.5 π mm mrad
Vertical Emittance	1.5 π mm mrad
Energy Spread	0.3 - 0.4%
Beam Size at Undulator Entrance	
Horizontal Size (FWHM)	1.2 mm
Vertical Size (FWHM)	0.5 mm
Macropulse Length	5 μs
Micropulse Repetition Frequency	2.8 GHz
Undulator	
Type	Planar Electromagnet
Period (Number of Periods)	25 mm (80)
Peak Magnetic Induction	4.8 - 6.8 kG
Gap Spacing	5.6 mm
Resonator	
Cavity Length	2781 mm
Cylindrical Mirror	R=3000 mm
Waveguide Gap	3.6 mm
Waveguide Length	2778 mm
Radiation Wavelength	100 - 200 μm
Optical Beam Waist (Horizontal Plane)	6.8 - 9.6 mm
Effective Optical Beam Size (FWHM)	
Horizontal Plane	8.2 - 11.6 mm
Vertical Plane	1..0 mm

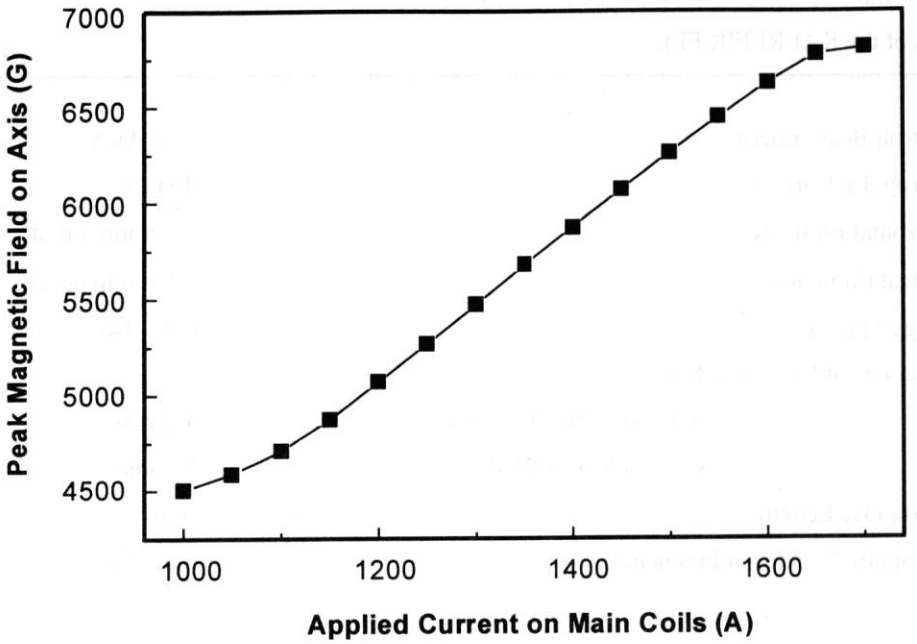

Fig. 1. Measured magnetic field strength of U25 undulator as a function of the applied current on main coils.

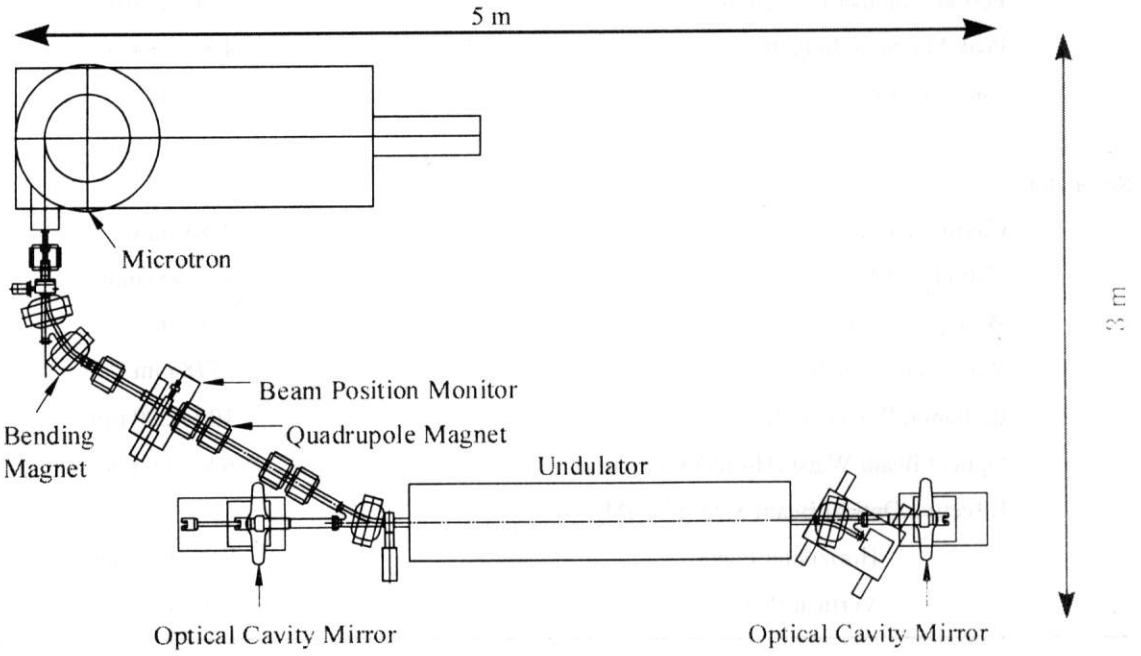

Fig. 2. Schematic of the compact FIR Free Electron Laser driven by a microtron.

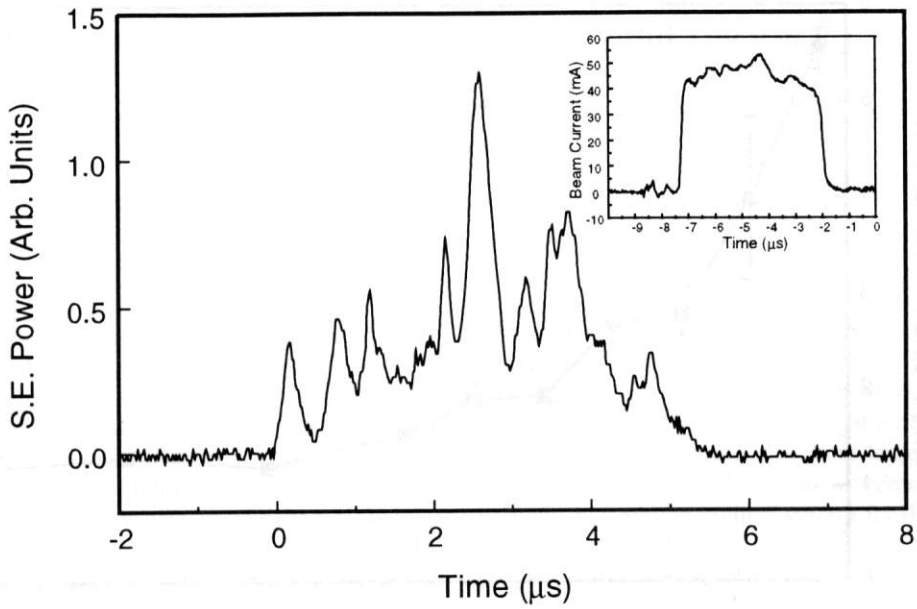

Fig. 3. Measured power of the spontaneous emission from the FIR FEL.

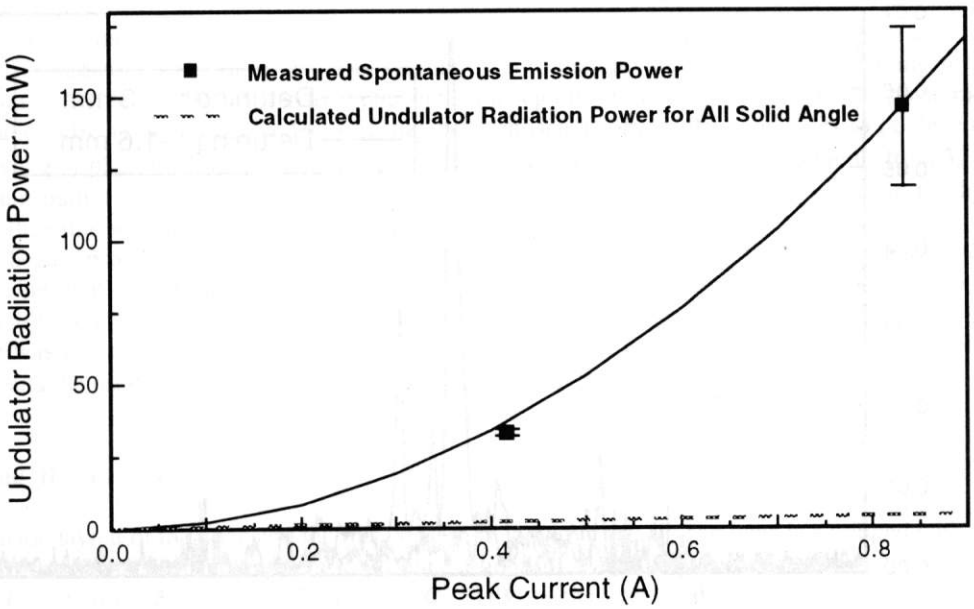

Fig. 4. Measured spontaneous emission power as a function of the beam current.

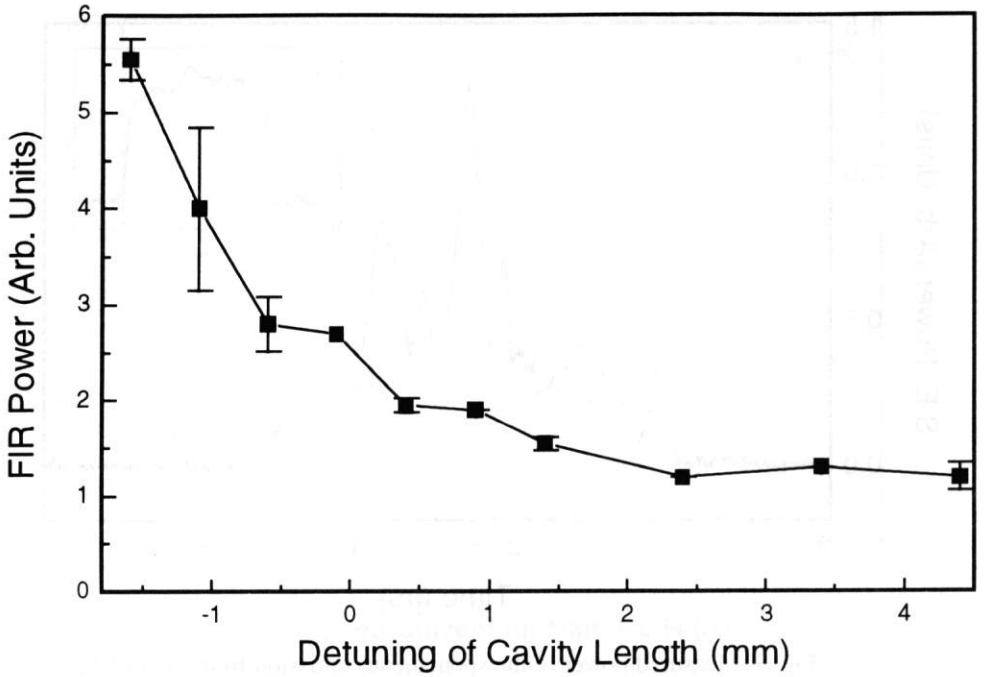

Fig. 5. Measured outcoupling radiation power from the FEL oscillator by changing the cavity length.

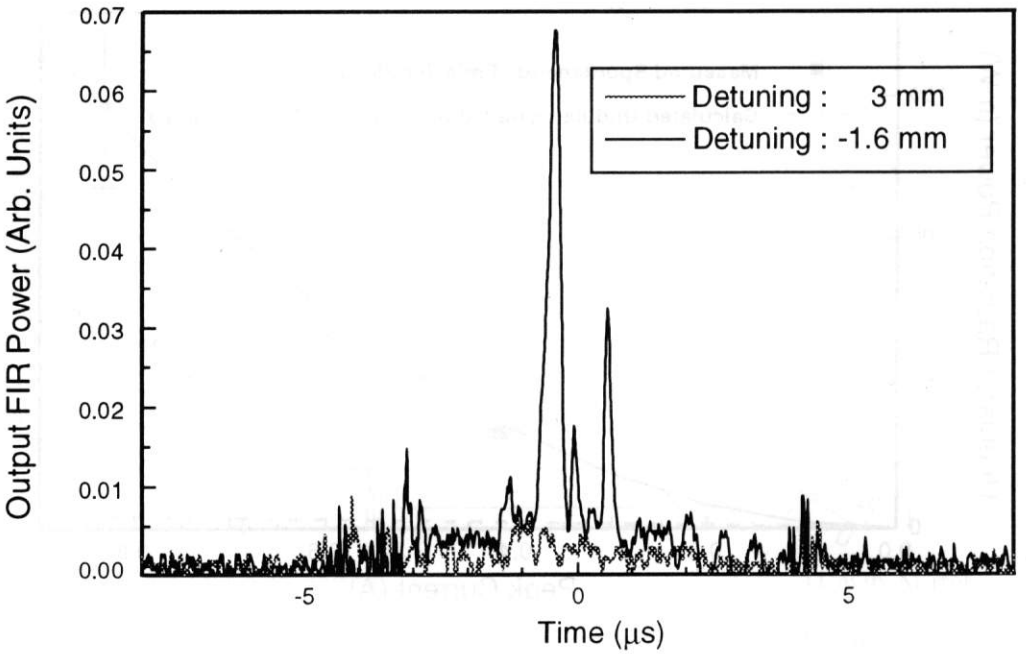

Fig. 6. Temporal evolution of the radiation power with the different cavity length.

High-Current 2-MeV Electron Accelerator for High-Power FEL

Byung Cheol Lee [1], Sung Oh Cho, Young Uk Jeong,

Sun Kook Kim, and Jongmin Lee

Korea Atomic Energy Research Institute (KAERI), P.O. Box 105, Yusong, Taejon, 305-600, Korea

Gennady N. Kulipanov

Budker Institute of Nuclear Physics, Lavrentyev ave., 11, 630090 Novosibirsk, Russia

Abstract : A high-current CW electron accelerator has been developed for the free electron laser (FEL) programs at KAERI under the cooperation of KAERI and the Budker institute of Nuclear Physics (BINP), Russia. The accelerator is composed of a 300-keV electron gun, a radio frequency (RF) buncher cavity, and two RF acceleration cavities. The kinetic energy of the electron beam is 1.5 MeV nominally and 2 MeV at maximum. The duration of a pulse is 350 ps and its repetition rate is variable from single pulse to 22.5 MHz. The peak current is 6 A, and the average current at maximum repetition rate is 50 mA. The resonant frequency of the normal-conducting RF cavities is 180 MHz. The accelerator will be used as an injector of a high-power infra-red free electron laser, and for e-beam processing of polymers, exhaust gas, waste water, power semiconductor etc..

1. Introduction

In order to drive a high average power free-electron laser (FEL), a high average current electron accelerator is indispensable. A recirculating radio frequency (RF) accelerator with energy recovery seems to be the best choice for this purpose [1-3]. One of the critical issues in the development of the recirculating accelerator with energy recovery is the generation of high-average-current electron beam with proper energy and good beam quality. The choice of accelerator structure, especially the type and the frequency of the RF cavity, is very important. Two high average current accelerators using super-conducting acceleration cavities have been in successful operation [4,5]. Recently, KAERI has finished installation and commissioning of a 2-MeV, CW, normal-conducting in corporation with BINP. The average current of the electron beam from the accelerator is 45 mA at maximum. The accelerator will be used as the injector for a high energy recirculating accelerator for a high power FEL.

2. The electron accelerator system

Figure 1 shows a schematic of the whole accelerator facility including the RF generator and the control system. Figure 2 shows a photograph of the accelerator. And Figure 3 shows a schematic of the accelerator system. The accelerator is composed of a 300-keV electron gun, one RF bunching cavity, two RF acceleration cavities, a 180-degree bending magnet, ad a beam dump. Main parameters of the electron

[1] Corresponding Author : T) 82-42-868-8378, F) 82-42-861-8292, E) bclee4@kaeri.re.kr

accelerator are listed in Table 1. The resonance frequency of the RF cavity is 180 MHz. The maximum repetition rate of the electron beam should be equal to the RF frequency divided by the number of turns and, in our design of FEL system, is ≈180 /8 = 22.5 MHz. The normalized emittance should be ε_n ~ 150π μm-rad in order to enable lasing at ~5 μm wavelength. The bunch length is 350 ps and the peak current is 6 A.

The electron gun is composed of a cathode-grid unit controlled by a modulator, a electrostatic linear accelerating tube placed in a high-pressure vacuum vessel with insulating SF_6 gas, a 300-kV DC power supply, a power supply for the high-voltage part of the gun with an isolation transformer, and control electronics with optical signal transmission to and from the high-voltage part. In order to get a very short pulse electron beam (1.5 ns) from the electron gun, we use a tetrode-type thermionic cathode. The cathode-grid unit operates in the space-charge-limited emission mode. The gap distance between the cathode and the grid electrode is 0.1 mm, and the voltages between the cathode and the grid is optimized to get minimum emittance of the electron beam. The emittance calculated by using a simulation code does not exceed 20 π μm rad. The pulse duration of 1.5 ns corresponds to an ≈100 degree of phase interval at the main accelerating (and bunching) frequency of 180 MHz. If the duration is larger, a significant number of electrons are lost during bunching. The main parameters of the electron gun are listed in Table 2.

The resonance frequency of the bunching RF cavity is 180 MHz [6]. The cavity has copper clad stainless steel walls. The Q value of the cavity is 42,000, and the shunt impedance is 8.5 Mohm. The tuning range of the resonant frequency is 320 kHz, and the tuning speed is 5 kHz/sec. The wall loss at a cavity voltage of 850 kV is 100 kW.

The RF power supplied into the bunching cavity is 2 kW, and the corresponding RF-voltage in the cavity is 110 kV. For the best bunching of the electron beam, the RF phase is chosen so that the energy loss of the electron bunch is 30 keV after passing the bunching cavity. Since the power lost by electrons is comparable to the RF power, the phase and the amplitude of RF in the cavity should be controlled very carefully.

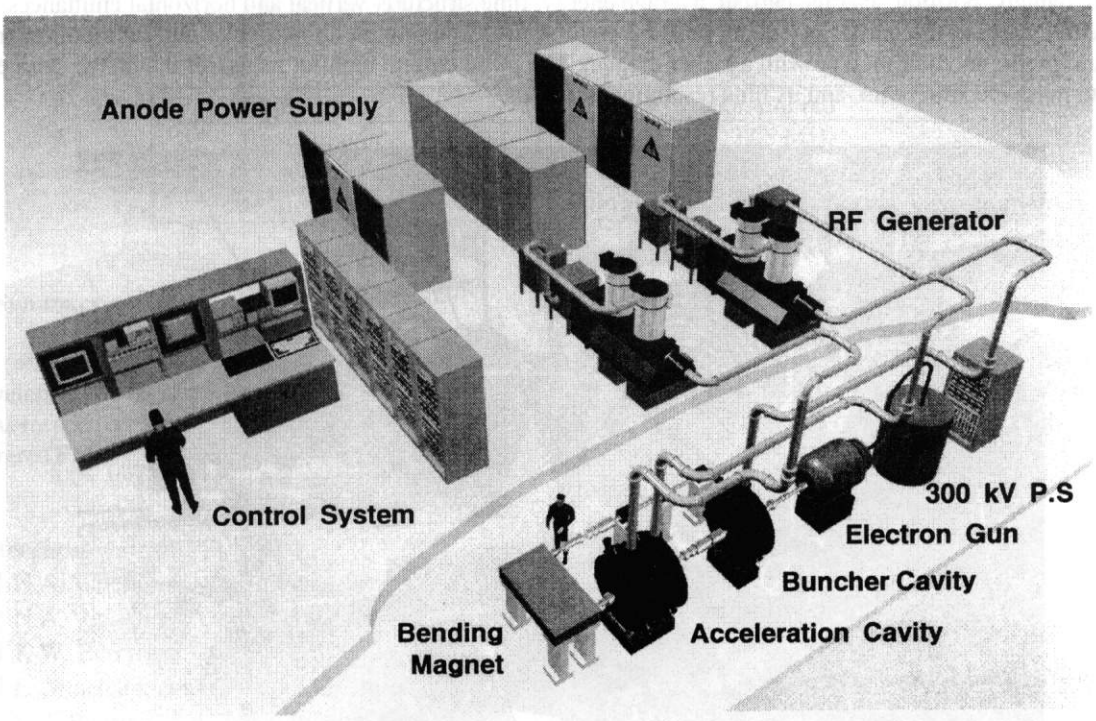

Fig 1. Schematic of the high-average-current 2-MeV electron accelerator facility

Table 1. Main parameters of the 2-MeV electon accelerator.

Electron energy (kinetic)	1.5 MeV (nominal) 2.0 MeV (maximum)
Current	6 A (peak) 45 mA (average)
Emittance	40π μm rad
Repetition rate	Single pulse ~ 22.5 MHz
Pulse duration	350 ps
RF frequency	180 MHz
Operation mode	CW

The main accelerating section is composed of two independently-controlled RF cavities. The accelerating cavities have almost the same structure and parameters as that of the bunching cavity. The energy gain from each accelerating cavity is 600 keV nominally, and 800 keV at maximum. The distance between the bunching cavity and the first accelerating cavity is chosen such that the bunching process occurs optimally.

The transport beamline is intended for guiding a beam through the vacuum chamber, minimizing emittance at the output of the injector, and fitting parameters of the beam to the recirculating main accelerator. It consists of sets of magnetic correctors, solenoidal lenses, quadrupole lenses, and a 180^0 bending magnet.

The beam measurement system is intended for measuring all the significant parameters of the electron beam, namely: position, average current, average energy, time structure, vertical and horizontal emittances, and energy spread. It consists of a beam position monitor; a DC current monitor; a pulse current monitor; and a beam profile monitor module with a kicker magnet. The pulse current monitor measures the image charge due to pulse electron beam, and its time resolution is 100 ps.

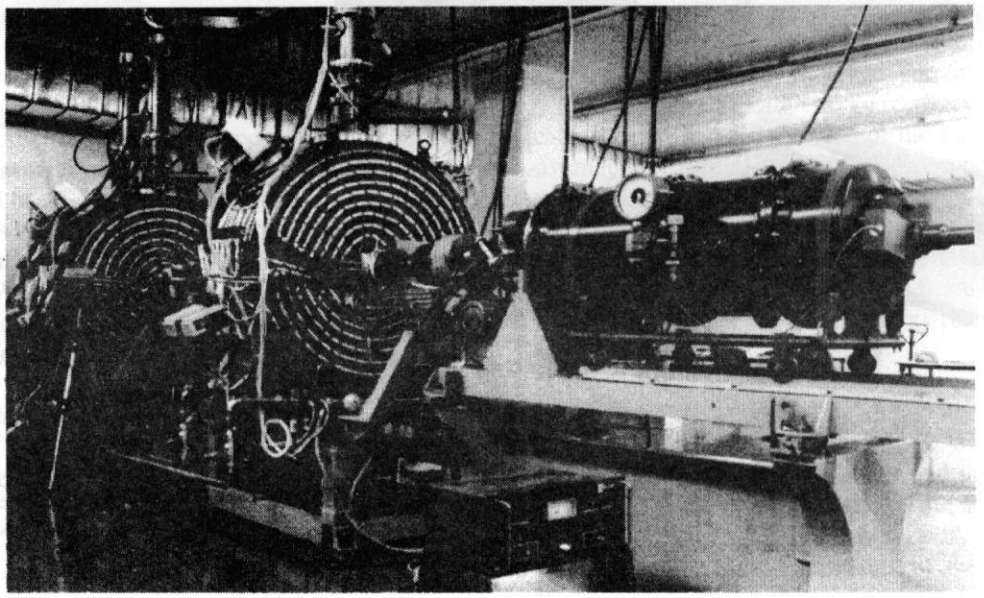

Fig 2. Photograph of the 2-MeV electron accelerator system

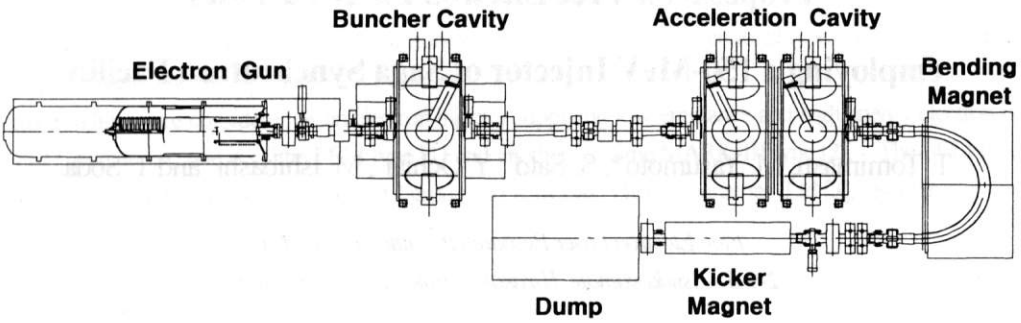

Fig 3. Schematic of the 2-MeV electron accelerator system

Simulations show that most part of a 1.5-ns pulse can be bunched to < 100 ps duration with an energy spread of less than 20 keV . The 'tails' laying out of 1.5 ns duration hardly can be bunched, and will be lost after passing the bending magnet due to large energy spread. At 1 MHz of repetition frequency, more than 95 % of the electron beam from the electron gun pass through the beamline and reach the dump. At 4 MHz of repetition frequency, the transport ratio decreases to 75 %, which seems to be related to the beam instability at high average current.

Table 2. Parameters of the 300-keV electron gun.

Electron energy (kinetic)	300 keV
Current:	1.25 A (peak) 45 mA (average)
Emittance	160π μm rad
Repetition rate	0...22.5 MHz
Pulse duration	1.6 ns
Operation mode	CW / Single pulse

3. Summary

A high-average-current CW electron accelerator using normal-conducting RF cavities has been developed and commissioned. The energy and the average current of the electron beam are 2 MeV and 45 mA, respectively. The accelerator will be used as an injector of a higher-energy accelerator for high-power infrared FEL.

References

[1] N.A. Vinokurov, *et al.*, Nucl. Instr. And Meth. A375, p403, 1996.
[2] N.A. Vinokurov, et al., LBNL-40081 UC414, March 1997
[3] K.W. Berryman, et al., SPIE Vol 2376, p53, 1995.
[4] E. Minehara, et al., Proc. of 19th International Conference on Free Electron Laser, II-45, Elsevier, 1998
[5] S.V. Benson, et al., Nucl. Instrum. and Meth. A 407, 401, 1998
[6] V.S. Arbuzov, et al., Proc. of the 1993 Particle Accelerator Conf., Vol 2, p1226, 1993

The Straight-Flight Cavity for Monitoring of Microtron Intrapulse Instabilities

*Grigori. M. Kazakevitch, Young Uk Jeong, Byung Cheol Lee, Sung Oh Cho, Sun Kook Kim and Jongmin Lee

**Budker Institute of Nuclear Physics, Lavrentyev av. 11, 630090, Novosibirsk, Russia.*
Lab. for Quantum Optics, Korea Atomic Energy Research Institute, P.O. Box 105, Yusong, Taejon, 305-600, Korea.

Abstract: It was 2.8 GHz straight-flight Cavity designed for investigation of the intrapulse frequency instabilit of the bunched beam in the entrance of submillimeter FEL, driven by the classical microtron. The Cavity is cylindrical, low Q-factor resonator with the coupling less than critical. Tuning system of the cavity driven b moving mechanism provides retuning in bandwidth +/_ 7.5 MHz. Design of the cavity admit to chang disposition of the coupling loop to choose and control the coupling coefficient. The geometrical aperture fo transportation of the electron beam through straight-flight cavity is 26 mm.

1. INTRODUCTION

Stability question of the bunches repetition rate during macropulse is very important for RF pulsed accelerator which are supposed to be used as a driving system for FELs, because noticeable instability of that lead to chang for the worse coherence of the radiation and in the end can be reason of decreasing of the gain in FEL resonator. For the monitoring of the bunch repetition rate instability during macropulse of the accelerator in compact far infrared FEL driven by microtron [1], a straight-flight monitoring cavity was designe manufactured, tested and mounted in the beam line of the FIR FEL installation.

2. THE MONITORING CAVITY DESIGN DESCRIPTION

Parameters of the cavity were determined to get more complete information about frequency properties of t bunched beam, passed through it. For this reason the Q-factor of the monitoring cavity was chosen less than t Q-factor of loaded acceleration cavity in the microtron. Geometrical aperture of the monitoring cavity was fou in correspondence with that of the beam line. The monitoring cavity was positioned in the end of first straig section of beam line of the FIR FEL installation, after first X-focusing quadruple lens. Output signal from t cavity lead out by coupling loop through coaxial N type connector. Connector have vacuum sealing. Throug coupling loop the monitoring cavity loaded by 50 Ohm cable line on the measuring equipment in a contr room. Oversimplified drawing of the straight-flight monitoring cavity is given in the Fig. 1.

For design of the monitoring cavity was used the simple in the manufacturing cylindrical construction f E (010) mode oscillation. Calculations of cavity parameters and sizes were made with recommendations

onograph [2]. For decreasing of Q-factor, the cavity body and it's covers were made from stainless steel. ıdium-wire sealings were used by the assemblage of the monitoring cavity and it's connection with beam line provide pure vacuum in all parts of the far infrared FEL installation. For the retuning of the frequency of onitoring cavity was designed the moving mechanism, which provide smooth shift of 2 mm diameter 60 mm ng two ceramic shafts along direction of the electric field in the monitoring cavity. Supports of ceramic shafts e clamped on the retuning mechanism support, which can shift smoothly by screw moving mechanism. Two) mm long flexible bellows welded on both ends of retuning mechanism support provide free moving of it in nge +/_8 mm. Coupling loop construction permit to change it disposition to choose and control the coupling efficient in range 0.12 - 0.54. Aluminum 0.4 mm thick window on the monitoring cavity output is transparent r accelerated electrons and permit to have targeting of the electron beam by the external scintillation screen nd centering of electron trajectory on the monitoring cavity axis too. Measurement of current of the electron eam, passed through monitoring cavity is available by Faraday cap. Nonius scale indicator of the moving echanism permit to get mechanical repeatability of ceramic shafts positioning with accuracy 0.1 mm. It rrespond repeatability of monitoring cavity tuning with accuracy about 100 kHz.

EXPERIMENTAL DATA

The straight-flight monitoring cavity was tested by usual RF methods. It was excited by RF generator rough coupling loop. The Precise Digital Hewlett-Packard ESG D3000A Generator was used for excitation in gime of the frequency modulation with frequency deviation 40 MHz. This mode of the operation guaranteed e high homogeneity for spectral distribution of the exciting signal and high accuracy by the measurement of e resonant curve. The Spectrum Analyzer Tektronix 2782 was used for investigation of the output RF signal probe. Vacuum sealed probe with coaxial output was installed on the monitoring cavity axis. Disposition of e probe was chosen to provide minimal coupling coefficient with monitoring cavity to avoid probe influence the cavity resonance frequency. Retuning curve of the cavity by the value of coupling coefficient with enerator about 0.5 is given in the Fig. 2. Graph show the resonant frequency shift for this monitoring cavity in pendence on the retuning mechanism indicator position. Full range of the retuning of monitoring cavity is 5 MHz. Measurements were done by real value of vacuum in the monitoring cavity. Frequency of the onitoring cavity by length: 0 mm correspond 2.8040 GHz. The Q-factor value of monitoring cavity is about 000 by indicated above value of the coupling coefficient.

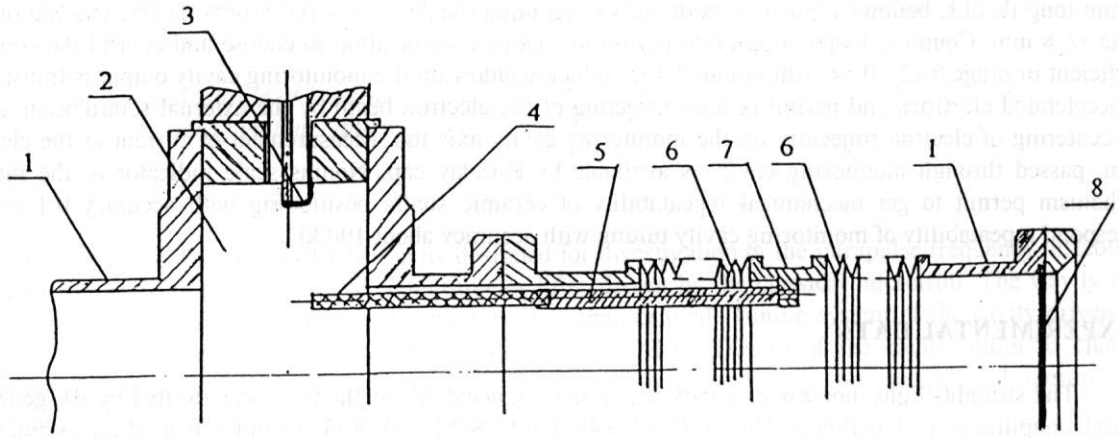

Fig.1. Straight-flight monitoring cavity. 1-beam line pipe; 2-monitoring cavity; 3-coupling loop; 4-ceramic shaft; 5-ceramic shaft support; 6-bellow; 7-retuning mechanism support; 8- output aluminum window.

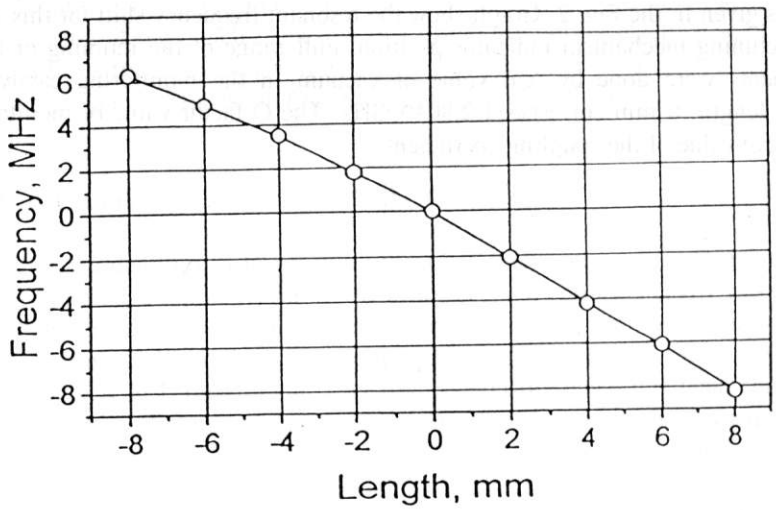

Fig.2. Retuning curve of the monitoring cavity.

REFERENCES:

[1] R.R.Akberdin, G.M.Kazakevitch, G.N.Kulipanov, A.S.Medvedko, S.V.Miginsky, S.F.Mikhailov, A.D.Oreshkov, V.M.Popik, G.I.Silvestrov, N.A.Vinokurov, P.D.Vobly, J.Lee, B.C.Lee, Y.U.Jeong, S.O.Cho. Nucl. Instr. & Meth. in Phys Res. A 405, 195-199, 1998.

[2] L.A.Vanstein. Electromagnetic Waves. Radio i sviaz. Moscow, 1988.

Measurements of Intrapulse Instabilities in the Electron beam of high Current Microtron

*Grigori. M.Kazakevitch, Young Uk Jeong, Byung Cheol Lee, Sung Oh Cho, Sun Kook Kim and Jongmin Lee

**Budker Institute of Nuclear Physics, Lavrentyev av, 11, 630090, Novosibirsk, Russia.*
Lab. for Quantum Optics, Korea Atomic Energy Research Institute, P.O. Box 105, Yusong, Taejon, 305-600, Korea.

Abstract: It was measured the intrapulse instability of the bunches repetition rate of the electron beam in the Far Infrared Free Electron Laser installation driven by microtron. For measuring was used the straight-flight monitoring cavity, which was mounted in beamline of the installation. The beam current of microtron was in range 35-55 mA by beam energy about 7 MeV and macropulse width about 5 μs. It was found, that repetition rate of bunches during macropulse have oscillations with period about 0,6-0,7 μs. In the same time, as was found, repetition rate of bunches have tendency to increase along macropulse width. In the first approachment this increasing depend by linear law on the increasing of emission current along macropulse. The constant of increasing of the bunch repetition rate is about 20 kHz/μs, amplitude of the frequency modulation is about +/_30 kHz for optimal conditions of microtron operation.

1. INTRODUCTION

The problem of stability of the electron bunches repetition rate during macropulse is major one for use RF accelerators as injectors in FEL installation. In case of use the classical microtron driven by magnetron generator this problem is most important. Driven by 2.8 GHz MI-456A tunable magnetron the compact microtron, which was chosen as injector of electron bunches in the compact Far Infrared FEL installation, was investigated in problem of intrapulse bunch repetition rate stability by straight-flight monitoring cavity [1].

2. EXPERIMENTAL INSTALLATION DESCRIPTION

The RF system of compact microtron [2] was chosen to provide additional stability of magnetron generator frequency. For this reason the microtron waveguide RF line was extremely short and ferrite insulator had opposite direction losses no more, than 15 dB. In this case accelerating cavity can provide additional stabilizing action on the magnetron generator by the reflected wave.
A 7 MeV electron beam with macropulse current in range 35-55 mA and macro pulse width about 5 μs was passed through monitoring cavity on the axis. The monitoring cavity was positioned in the first straight section of beamline of FIR FEL installation, as sown in the Fig.1. Electron beam was centered

on the axis of monitoring cavity by external scintillation screen and dumped in the Faraday cup in output of the cavity. RF signal was arisen due to excitation of the monitoring cavity by bunched electron beam. Outcoupled RF signal was feed by 50 Ohm cable line in the control room and was mixed by M8TS mixer with heterodyne signal from precise Hewlett-Packard ESG D3000A Digital Signal Generator. The frequency difference signal was measured by 2 GS/s LeCroy 9374 oscilloscope. Uncertainty of this measurements in determination of the beginning of the frequency difference signal is no more, than 0.25 μs. The small negative detuning of the magnetron generator was chosen to provide essential accelerated current in the range 35-55 mA by the minimal value of the bunch repetition rate deviation during macropulse of the microtron.

3. EXPERIMENTAL RESULTS

Typical oscillograph record of the change of the bunch repetition rate during macropulse for the frequency difference about 8 MHz and emission current in microtron about 1.1 A is shown in the Fig.2. The middle peak can be explained owing to some discoupling of the microtron modulator storage line for magnetron current less then optimal. This peak can be decreased by optimization of the magnetron current, Fig. 3.

Dependence of increasing of the bunch repetition rate during macropulse of beam was investigated for different operation condition of the microtron, including experiments with different value of magnetron generator detuning. It was found, that constant of increasing is about 20 kHz/μs in optimal condition of microtron by accelerated current about 50 mA. It was found too, that the constant of increasing of the bunch repetition rate increased with the growth value of emission current during macropulse in linear law at first approachment.

This phenomena can be explained by the inlinearity of oscillation in the microtron accelerating cavity. Source of the inlinearity is the interaction between electromagnetic field of the electron beam and electromagnetic field in the cavity [3], [4]. Analysis of oscillograph records by the frequency difference in the range 4-12 MHz showed the frequency modulation in the range about +/_ 30 kHz for optimal conditions of microtron operation with accelerated current about 40-50 mA. The frequency modulation effect can be explained by the interaction of the bunch electromagnetic field and electromagnetic field in the acceleration cavity of the microtron too. It's important to add, that the value of the frequency modulation amplitude depend on the magnetron generator detuning and additional increasing of detuning of the magnetron generator in our RF system lead to increasing of the amplitude of the bunch repetition rate frequency modulation during macropulse of the electron beam. Value of the frequency modulation amplitude about +/_30 kHz correspondent of the minimal detuning which provide accelerated current about 50 mA.

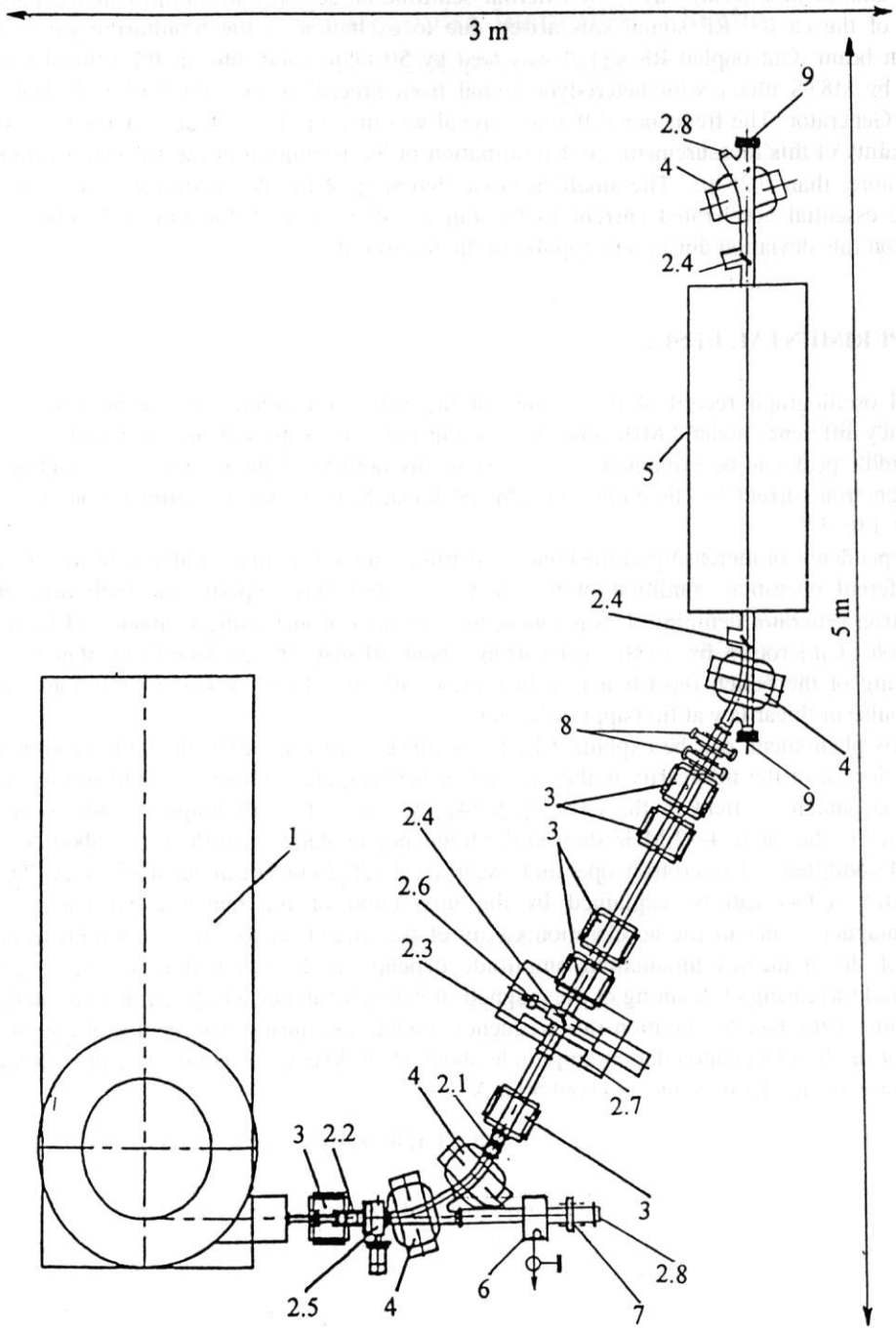

Fig.1. Layout of the FIR FEL installation. 1-microtron; 2.1, 2.2-bellows; 2.3 ceramic tube; 2.4-OTR screen; 2.5-valve; 2.6- OTR chamber; 2.7-beam current transformer; 2.8-aluminum output window; 3-quadruple lens; 4-bending magnet; 5-undulator; 6-straight-flight monitoring cavity; 7-moving mechanism; 8-X - Y steering magnet; 9-FIR resonator flange.

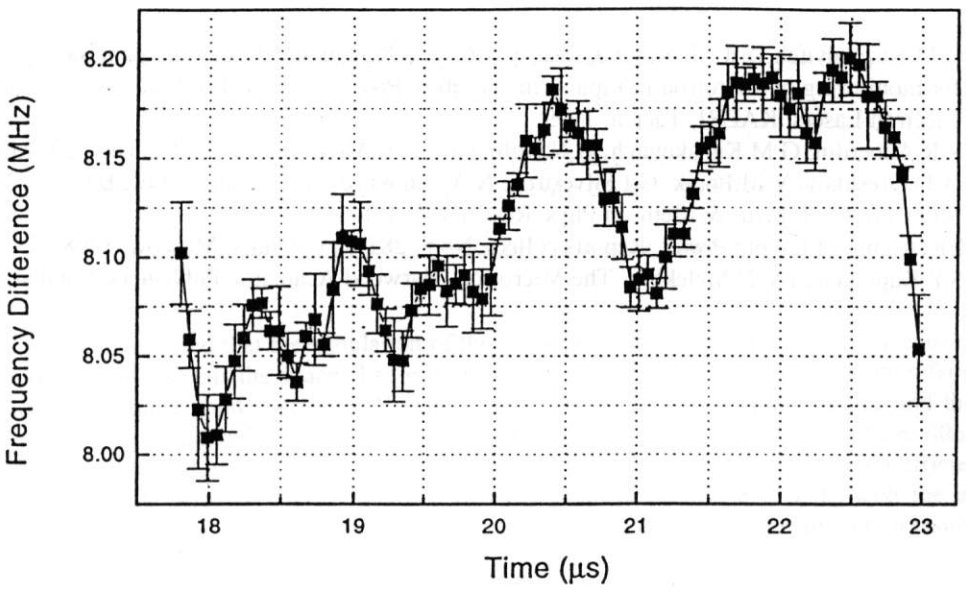

Fig.2. The change of the bunch repetition rate frequency during macropulse current. Front of beam pulse begin at 17.5 μs. The heterodyne frequency is 2.794 GHz.

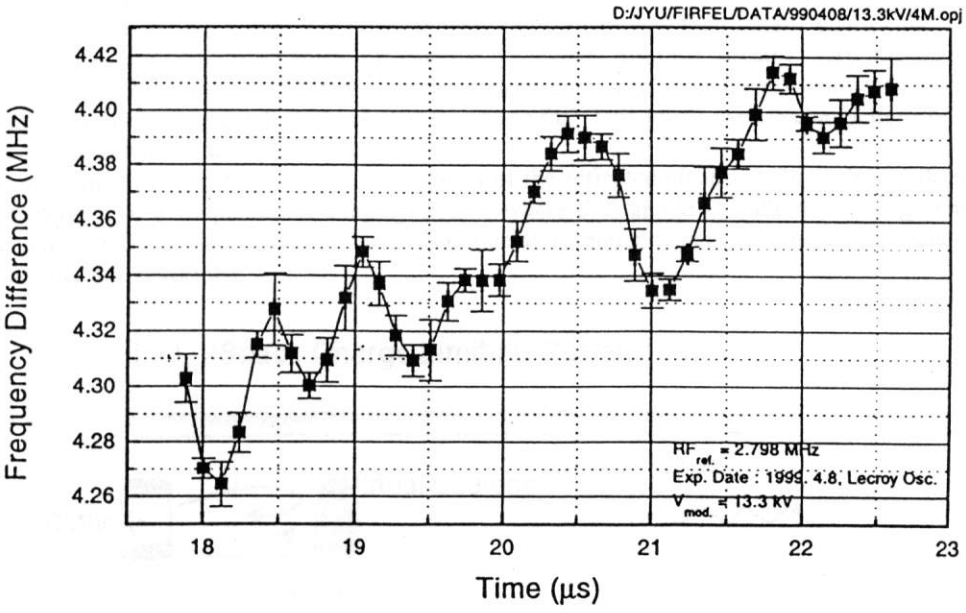

Fig.3. The change of the bunch repetition rate frequency during the macropulse by optimal pulse current of the magnetron. Microtron emission current is about 1.4 A. Front of beam pulse begin at 17.5 μs. The heterodyne frequency is 2.798 GHz.

REFERENCES:

[1]. G.M.Kazakevitch, Y.U. Jeong, B.C.Lee, S.O.Cho, S.K.Kim and J.Lee. The straight-flight cavit for monitoring of microtron intrapulse instabilities. Proceed. of the 4th Asian Symposium on Free Electron Lasers, KAERI, Taejon, 1999.

[2]. R.R Akberdin, G.M.Kazakevitch, G.N.Kulipanov, A.S.Medvedko, S.V.Miginsky, S.E.Mikhailov, A.D.Oreshkov, V.M.Popik, G.I.Silvestrov, N.A.Vinokurov, P.D.Vobly, J.Lee, B.C.Lee, Y.U.Jeong, S.O.Cho. Nucl. Instr. & Meth. in Phys. Res. A 405, 195-199, 1998.

[3]. Electronics of the big Power. Reports collect. No 5, 283-305, Nauka, Moscow, 1968.

[4]. S.P.Kapitza and V.N.Melekhin. The Microtron, Harwood Academic Publishers, London, 1978.

The Orbit Design of the Accelerator-Recuperator for the Free Electron Laser.

E.I. Antokhin, D.A. Kairan[1], V.G. Tcheskidov, N.A. Vinokurov, P.D. Vobly.

Budker Institute of Nuclear Physics
11 Ac. Lavrentyev Prosp., 630090, Novosibirsk, Russia

Abstract: The special requirements for the magnetic system of the accelerator-recuperator are considered. The solution, which meets these requirements, is found. Some results of the lattice design are described.

1.Introduction

Like all accelerators the accelerator-recuperator [1,2] is used for acceleration the charge particles to high energy. The motion of particles in accelerator-recuperator has the important feature: the electrons after the acceleration in the RF-cavities to the necessary energy are returned to the RF-cavities in the decelerating phase and give the energy back. The energy recuperation offers the low injection and ejection beam energy, which is preferable for radiation hazard reduction. The energy recuperation is also useful to decrease the required power of the RF-generators. The use of multiple passes through the accelerating section [3,4] reduces further the RF power and the number of the RF-cavities also.
One of the most attractive applications for accelerator-recuperators is a free electron laser. The Budker Institute of Nuclear Physics with the Institute of Chemical Kinetics and Combustion keep the construction of the High Power Free Electron Laser for the Siberian Center of Photochemical Research. The general scheme of the FEL on the base of the accelerator-recuperator is shown in Fig. 1.

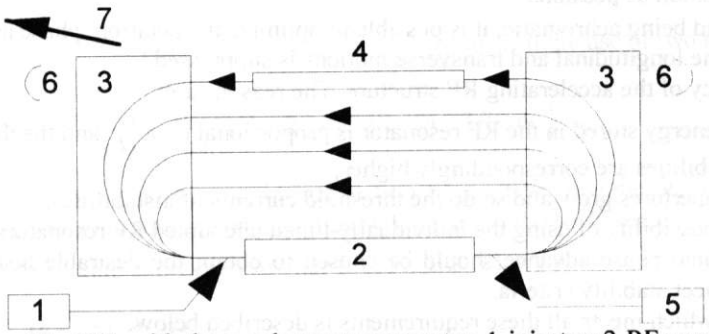

Fig. 1. The scheme of the FEL with the accelerator-recuperator. 1-injector; 2-RF accelerating structure; 3 -180-degree bends; 4-FEL magnetic system; 5-beam dump; 6-mirrors; 7 output light beam.

2. The electron beam motion in the accelerator-recuperator

Let us consider the motion of the electron beam in the accelerator-recuperator in more detail. The beam leaves the injector (1), and passes the common straight-line accelerating section (2) of the accelerator-

[1] Corresponding author. Tel: +7-3832-394003, Fax: +7-3832-342163, e-mail: kairan@inp.nsk.su

recuperator. Leaving the accelerating structure, the electrons pass two 180-degree achromatic bends (3) and return to the accelerating structure (1) ones more.

The beam always to come in the accelerating phase, the length of the orbits has to be a multiple of λ, the wavelength of the accelerating voltage. Since an increase of energy leads to an increase of the bend radius in the magnet and, consequently, an increase of the orbit length, the difference between the preceding orbit and the succeeding one is to be also a multiple of λ. In the design under consideration this difference was chosen equal to λ.[2]

After the necessary number of the passes through the accelerating structure the electrons come to the user's magnetic system (in our case we are going to use the beam in the free electron laser magnetic system (4)), where they may get an additional energy spread. The length of the last orbit is chosen so that returning to the resonators, the electrons get into the decelerating phase of the RF voltage and return the energy to the resonators. The process of deceleration looks similar to the acceleration. When the beam energy become almost the injection energy the beam is deflected to the beam dump (5). Due to the low energy of the electrons to be dumped no neutron generation occurs in the beam dump and gamma-radiation of low energy is easily absorbed by a relatively simple shielding.

The following specific requirements to the magnetic system of the accelerator-recuperator may be pointed out.

I. Energy of the exhaust electrons (therefore, of the injected ones, too) should be lower than 10 MeV in order to avoid neutron generation.

II. The electron-optical system should provide proper focusing of beams both under acceleration and under deceleration. It is not easy, since in the straight line sections there is simultaneously a beam under acceleration and a beam under deceleration. But the most complicated section is the common straight section, where the accelerating RF structure is situated. In the common section there are simultaneously 2N (N is the number of passes through the linac during acceleration) beams of different energies and with different initial conditions.

III. Energy acceptance should be a large enough (several percents). This requirement is a critical one because after passing the magnetic system of the FEL the electron beam gets an energy spread up to several percents. To return the beam to the beam dump successfully, the transverse dispersion should be as small as possible.

IV. The 180° bend being achromatic, it is possible to optimize the betatron phase and the linear coupling of the longitudinal and transverse motions is suppressed.

V. Low frequency of the accelerating RF structure. The reasons are:

   A. the energy stored in the RF resonator is proportional to λ_{RF}^3 and the threshold currents of instabilities are correspondingly higher;

   B. the apertures grow and so do the threshold currents of instabilities;

   C. the possibility of using the individually-tuned uncoupled RF resonators.

VI. The longitudinal phase advance should be chosen to obtain the desirable beam parameters in the FEL and to meet stability criteria.

The magnetic system which meets all these requirements is described below.

3. 180-degree achromatic bends

It is critical in the realization of the bends that there is one magnet, common for all the passes, which performs separation of the orbits and there are magnets, different for different orbits, which add the

---

2 The sole exception is the last orbit, which is to be of a certain length to provide that the electrons return, after they passed it, in the decelerating phase, i.e. to differ from the last but one orbit by approximately $3/2\lambda$.

bend to 180 degrees. In the first four paths the rest bending system consists of one magnet. To solve the focusing problems, the bends from the fifth one contains two equal magnets. The last bend contains a 15-degree magnet and two equal magnets.

3.1 The bend with two magnets

To start with, we'll consider the geometry of the 180° bend, consisting of a round magnet and one bending magnet, of the same bend radius. The bend scheme is shown in
Fig. 2, where R is the bend radius of the magnets, a -radius of the round magnet, d - distance between the axis of the common straight section and the center of the round magnet, h - height of the path, $(\pi-\alpha)$ - angle of a bend by the first magnet. Simple geometrical consideration leads to the expression for the bend in the round magnet

$$\tan\frac{\alpha}{2} = \frac{R-d}{\sqrt{a^2-d^2}}. \qquad (1)$$

The distance between the round magnet and the second one is $l_0 = \frac{h-2R}{\sin\alpha}$. Then the total length of the orbit with the bend is

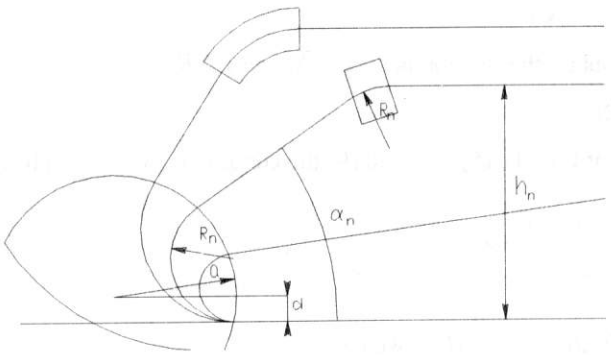

Fig. 2. Scheme of the 180° bend with the use of two magnets.

$$S = 2L + 2\left(\pi R + \frac{h-2R}{\sin\alpha} - \frac{h-2R}{\tan\alpha}\right) = 2L + 2\left(\pi R + (h-2R)\tan\frac{\alpha}{2}\right), \qquad (2)$$

where L is the length of the common straight-line section. One can see that the first term $2L$ will be the same for all the orbits, therefore the further consideration will be devoted only to the terms connected with the bends $s = S - 2L$. Substituting expression for $\tan\frac{\alpha}{2}$ (1) to Eq. (2), we have:

$$s = 2\pi R + 2\frac{(h-2R)(R-d)}{\sqrt{a^2-d^2}}. \qquad (3)$$

Until now we were considering only one orbit. Now we will compare the different orbits. As the energy increases linearly with the number of orbit and the bend radius in the magnet is $R = pc/eH$, the bend radius at the n-th pass will be

$$R_n = (n+\delta)\Delta R \qquad (4)$$

δ appeared due to the non-zero initial momentum ($\delta = p_0 / \Delta p$, where p_0 - the injection momentum, Δp

- the momentum gain per a pass). For the sake of convenience we shall consider the long straight parts of orbits to be located at an equal distance Δh from each other . Then the height of the n-th path is:

$$h_n = h_0 + n\Delta h \tag{5}$$

Substituting expressions for R_n and h_n to Eq. (3), one have:

$$s_n = 2\pi(n+\delta)\Delta R + 2\frac{(h_0 + n\Delta h - 2(n+\delta)\Delta R)((n+\delta)\Delta R - d)}{\sqrt{a^2 - d^2}}. \tag{6}$$

The difference of the lengths of passes n+1 and n :

$$\Delta s = s_{n+1} - s_n = 2\pi\Delta R + 2\frac{(d - 2R_n)(2\Delta R - \Delta h) - \Delta R(2R_{n+1} - h_{n+1})}{\sqrt{a^2 - d^2}}. \tag{7}$$

The particles to come in the same phase at each pass, the difference between passes n+1 and n should not depend on n and should be equal to λ.

$$\frac{\partial \Delta s}{\partial n} = -4\frac{\Delta R(2\Delta R - \Delta h)}{\sqrt{a^2 - d^2}} = 0 \tag{8}$$

From Eq. (8) we obtain the relation between Δh and ΔR

$$\Delta h = 2\Delta R. \tag{9}$$

Taking into account Eq. (4), (5), (7), and (9),the condition $\Delta s = \lambda$ can be represented in the form

$$\Delta s = \Delta h\left(\pi + \frac{h_0 - \Delta h\delta}{\sqrt{a^2 - d^2}}\right) = \lambda . \tag{10}$$

Resolving Eq. (10) for $\sqrt{a^2 - d^2}$, we have:

$$\sqrt{a^2 - d^2} = \frac{h_0 - \Delta h\delta}{\frac{\lambda}{\Delta h} - \pi}.$$

(11)

For our project the momentum increase per one pass through the accelerating resonators Δpc is 12 MeV and the injection momentum pc_0 is 2 MeV, then $\delta = 1/6$. Choosing the Δh and h_0 to have enough room between parallel straight-line sections, and the angle α_1 for the first orbit, one can find R_n, a, α_n and l_{0n}. Thus, we calculated the whole geometry of the 180 degree turns.

3.2 The bend with three magnets

To provide achromatism of the bend, the focusing elements are placed in the intervals between the magnets. Unfortunately, from the fifth path the distances between the axes of adjacent paths are small. It seems impossible to place there quadrupole lenses with large enough apertures. To solve this problem, on paths five to seven the second bending magnet is divided into two equal magnets with a bend radius twice smaller than that of the round magnet (see Fig. 3). The consideration, similar to the described above, but more awkward, gives us all necessary parameters.

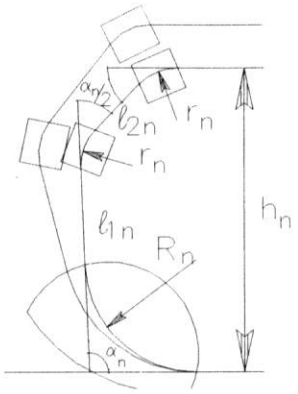

Fig. 3. Scheme of the 180° bend with use of the three magnets.

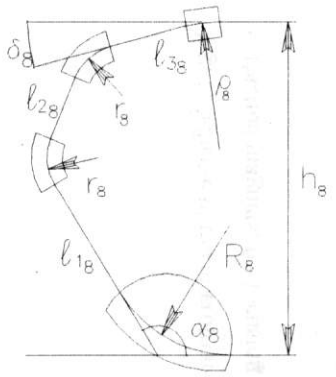

Fig. 4. Scheme of the 180° bend with use of the four magnets.

3.3 The bend on the eighth path with four magnets

The eighth path is special. Firstly, its length should be such that the particles, having passed it through, come to the resonators in the decelerating phase. And, secondly, the interaction with the radiation in the free electron laser take place in this orbit. So the last bending magnet of the 180-degrees turn must have large enough aperture to pass the FEL light through it. Therefore we divided the last 180 degrees turn on four bends: in the main round bending magnet, in the two equal bending magnets, and in the last large aperture bending magnet (see Fig.4).

The full scheme of the accelerator-recuperator is shown in Fig. 5[3], the main parameters of the magnetic system are presented in Table 1.

Energy	98 MeV
Magnetic field in the bending magnets	1.95 kGs, 3.90 kGs
Wavelength	166.182 cm
Length of common straight-line section	1995.48 cm
Distance between the common straight-line section and the last straight-line section	428.95 cm

Table 1. The main parameters of the accelerator-recuperator magnetic system.

References

[1] *V.G. Vesherevich et al.* The Project of Trace-Rack Accelerator-Recuperator for Free Electron Laser. Preprint BINP 90-82, Novosibirsk, 90.

[2] *G.I. Erg et al.* The Project of High Power Free Electron Laser Using Race-Track Accelerator-Recuperator. Preprint BudkerINP 93-75, Novosibirsk, 1993

[3] *R..E. Rand.* Recirculating Electron Accelerators. Harwood Academic Publishers, 1984.

[4] *N. A. Vinokurov, A. A. Zholents, W. M. Fawley and K.-J. Kim* Critical Issues for High-Power FEL Based on Microtron Recuperator/Electron Out-Coupling Scheme. Proc. of SPIE vol.2988 P.221-231, 1997.

[3] Making calculation of the orbit for the real bend we took into account the finite length of the round magnet edge. The maximum path length correction (for first path) is less than 0.2 mm.

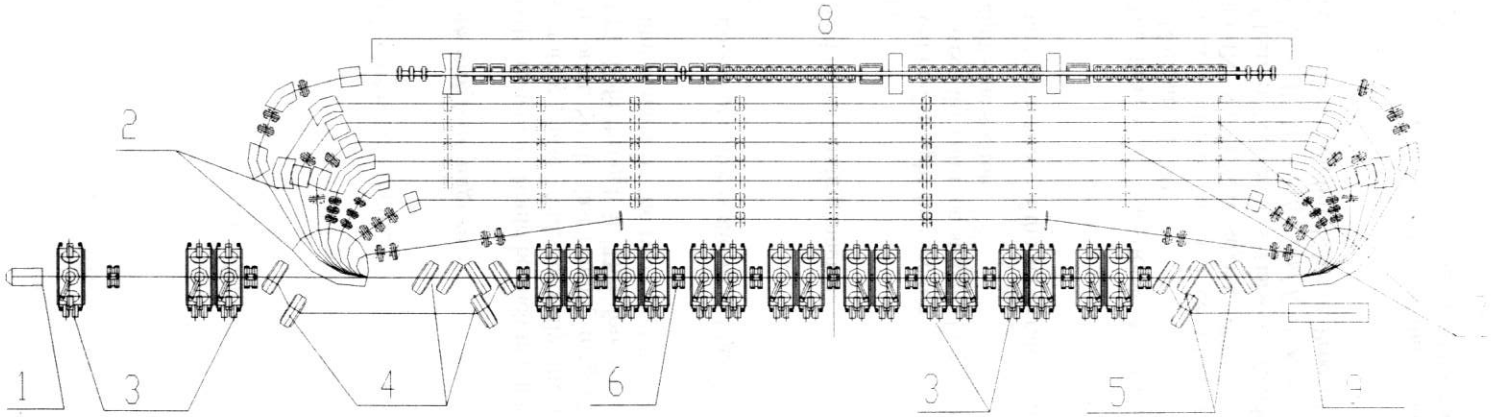

Fig. 5. Scheme of the microtron-recuperator (1 - electron gun; 2 - bending magnets; 3 - RF resonators; 4,5 - injection and extraction magnets; 6 - focusing quadrupoles; 7 - straight sections with the quadrupole lenses; 8 - FEL magnetic system; 9 - beam dump).

Selective Properties of Planar Resonators with 1-D and 2-D Feedbacks for Microwave FEM

An Yen Huan, A.V.Arzhannikov[1], E.V.Diankova[b], N.S.Ginzburg[a], P.V.Kalinin, N.Yu.Peskov[a], P.V.Petrov[b], S.L.Sinitsky, V.D.Stepanov

Budker Institute of Nuclear Physics, Novosibirsk, 630090, Russia
[a]Institute of Applied Physics, N-Novgorod, 603600, Russia
[b]RENC-VNIITF, Snezhinsk, 456770, Russia

Abstract: This paper describes selective properties of planar reflectors consisting of 1-D or 2-D Bragg gratings. It was turned out that mode transformation on a thread of the gratings had influence on a width of the spectral interval of the reflected radiation. Reflectors with chessboard or round-holes corrugation of gratings were proposed for the most effective 2-D distributed feedback.

1. Introduction

In order to generate 4-mm radiation in a narrow spectral band a planar resonator consisting of a regular wave-guide and two selective reflectors was used at the ELMI-device (BINP, Novosibirsk). Such reflector is constructed of two parallel Bragg gratings, which are manufactured of a copper plate with a small corrugation on its surface. Selective properties of this resonator determine the wave structure and the bandwidth of the generated radiation. It is well known that if e.m.-wave is scattered on the gratings then a reflected wave should satisfy to a Bragg resonance requirement:

$$\bar{k}_i - \bar{k}_s = \bar{k}\,, \tag{1}$$

where $\bar{k}_i$ and $\bar{k}_s$ - longitudinal wave vectors of impinging and scattered waves accordingly, $\bar{k}$ - wave vector of the corrugation on the gratings ($|\bar{k}| = 2\pi / d$, d is the corrugation period). For 1-D gratings the wave vector of the corrugation and one of the impinging wave are directed in the same directions, so the scattered wave is a backward to the impinging one. If it is necessary to have the impinging and the scattered back waves of the same mode and frequency, it should be $\bar{k} = 2\bar{k}_i$. The wave vectors for 2-D grating are directed at ±45° angles to the impinging wave and as a result, streams of energy in the transverse direction to the electron beam can be produced. These streams synchronise radiation of different parts of the electron beam so permitting to obtain a single mode regime of the wave generation.

In the first series of experiments with the FEM driven by a sheet beam the one-dimensional reflectors were used [1]. In this series the FEM produced 4-mm radiation with 200J total energy content at pulse duration of a few microsecond. For reaching a single mode operation of the generator at the ELMI-device the one-dimensional Bragg gratings were replaced by two-dimensional ones.

In the sections below studies of selective properties of the reflectors used in the experiments at the ELMI-device will be described. As a main result of these studies we have designed 2-D gratings with two types of the corrugation that will allow us to obtain the most effective 2-D distributed feedback for the further development of the experiment.

[1]Corresponding author. Tel: +7-3832-39-49-12, Fax: +7-3832-34-21-63, e-mail: arzhannikov@inp.nsk.su

2. 1-D reflectors.

One-dimensional gratings allow one to select radiation with a chosen wavelength. The corrugation thread for these gratings is made on a co-ordinate that is perpendicular to the direction of the wave propagation in a wave-guide. If the thread depth depends on a co-ordinate along the axis of the wave-guide under the harmonic law, there is only one spatial wave vector in the Fourier-decomposition of the Bragg grating surface. For this case the frequency of the reflected radiation is in a narrow bandwidth near to the frequency of the precise Bragg resonance. However, manufacturing such harmonic surface has some technological difficulties. As a rule, the gratings with rectangular shape of the threads are used. In this case the spectrum of the natural wave vectors for these gratings can be found from a Fourier-decomposition of lateral view of the thread (Fig.1).

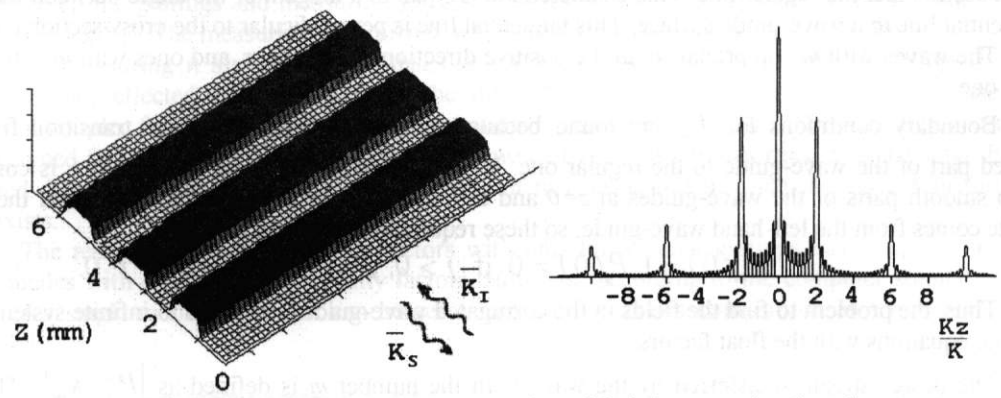

Fig.1. One-dimensional Bragg grating with the rectangular thread.

For definition of spectral properties of the Bragg reflectors some computer simulation was carried out. By this simulation we got the dependence of the reflectivity of these units on the incident radiation frequency at a different depth of the thread and at various length of the corrugation. For solving of this problem we used a method of the cross-sections [2]. This method is quite widely applicable for the wave-guides of slowly variable cross-section. Within the framework of this method the wave-guide with corrugated walls is determined as an irregular wave-guide with varying cross-section. The basic idea of the method is that the e.m.-field in any cross-section of the wave-guide is composed by superposition of the electromagnet waves running in two opposite directions in an auxiliary, rectilinear, regular wave-guide of the same cross-section:

$$\begin{cases} E_j = \sum_{m=-\infty}^{\infty} P_m E_j^m, \ j = x, y, z. \\ H_j = \sum_{m=-\infty}^{\infty} P_m H_j^m. \end{cases} \tag{2}$$

Decomposition values $P_m(z)$ in the expression (2) can be interpreted as the amplitudes of waves existing in our corrugated wave-guide. Substituting components of the e.m.-field given by expressions (2) into Maxwell equations it is possible to receive combined equations for values $P_m(z)$:

$$\frac{\partial P_m}{\partial z} - ik_m P_m = \sum_{n=-\infty}^{\infty} S_{mn} P_n. \tag{3}$$

The coefficients S_{mn} are termed as wave coupling coefficients, because they quantity characterise transformation of one waves to others by irregularity of the wave-guide. For the wave-guide with a varying cross-section these coefficients are given by expression:

$$S_{jm} = \frac{1}{2k_j(k_j - k_m)} \oint \nu(s)\left(E_n^j E_n^m + H_z^j H_z^m - H_s^j H_s^m\right) ds. \quad (4)$$

The unit vector s is tangential to a contour S on which the wave-guide wall and the cross-section plane are intersected. The basis vector n is perpendicular to s. It lays in the transverse cross-section plane and is directed to the wall of the wave-guide. The vectors n, s and z must form the right triple. The integral is taken contoured S. The function $\nu(s)$ is the characteristic of the difference between the corrugated wave-guide in the given section and the regular one. This characteristic is equal to a tangent of the angle between the axis z and tangential line to a wave-guide surface. This tangential line is perpendicular to the cross-section contour.

The waves with $m > 0$ propagate in the positive direction of the axis z, and ones with $m < 0$ - in the negative one.

Boundary conditions for P_m are found because of field's continuity at the transition from the corrugated part of the wave-guide to the regular one. If the corrugated part with the length L is connected with two smooth parts of the wave-guides at $z=0$ and $z=L$ and a wave with the number m and the single amplitude comes from the left-hand wave-guide, so these requirements look like:

$$P_m(0) = 1, P_j(0) = 0 \text{ if } j > 0, j \neq m; P_j(L) = 0 \text{ if } j<0. \quad (5)$$

Thus, the problem to find the fields in the corrugated wave-guide is reduced to infinite system of the differential equations with the float factors.

The power stream transferred by the wave with the number m is defined as $\left|P_m^2 / k_m\right|$. The total reflected power is accordingly equal to $\sum_{m=-\infty}^{0} \left|P_m^2 / k_m\right|$.

At preliminary calculations of a reflectivity it was supposed that the impinging and reflected waves belong to the basic type H_{10} and opportunity of the transformation of such wave by the gratings in waves of other types was not regarded. In such case, for the selected operational frequency 75 GHz the period of the thread was made 2mm, according to a requirement (1). Depth of thread and length of gratings were selected on results of computer simulations so that reflectivities of the input (at upstream side of the beam propagating in the channel) and output reflectors had values 95% and 75% respectively. For depth of the thread 0,2mm these lengths have to be equal 18cm and 10cm respectively.

The Bragg gratings with such parameters were manufactured. To check out the spectral properties of the reflectors a measuring bench was designed and constructed. As a basic element of the bench a Panoramic measurer of standing wave and impairment was used. The measurer consisted of a generator with frequency varied in the band 53,5-78,8 GHz and an indicator of mm-wave power. The indicator contained the oscilloscope tube for visually observation of frequency spectrum.

The reflectivity measuring was carried out by using two different schemes. In the first scheme the radiation from the generator comes to a parabolic mirror formatting a flat wave front. This wave goes through the reflector composed by the Bragg gratings and then it propagates through a converting plane horn. After that the wave comes to the detector registering the passed power. The signal from the detector is applied to the indicator and on its screen one can see a spectrum of the signal passed through the reflector. For definition of an absolute value of the reflector transmittance the directional coupler with the mm-wave detector are used. With its help the quantity of impinging power is measured. Knowing the impinging and passed powers it is possible to calculate the reflectivity of the reflector.

The other scheme is intended for immediate measuring of the reflected power. The radiation from the generator is transported to the reflector through the plane horn. To avoid the wave reflection from the unclosed exit of the reflector a dumping wave matter fulfils its output. This matter is porolon impregnated by graphite that accumulates the passed power of the mm-radiation. Two directional couplers with detectors are used for measuring of the impinging and reflected power.

Comparison of measured reflectivities for manufactured reflectors with results of computer simulations showed that these data were essentially differ both on absolute values, and on spectral behaviour. To vanish this differ the opportunity of the waves transformation from one type to another was taken into account in the computer calculations. It turned out that at presence of the wave-guide walls corrugation the wave H_{10} might effectively transfer to the wave E_{12}. This process gave additional increasing of reflectivity and expansion of the reflected spectrum band. The results of calculations with taken into account the mode transferring on the gratings and measuring for reflectivities (R) of two reflectors with different lengths are compared in a Fig.2. The measuring was carried out on the first scheme presented in the Fig.2.

By measuring it also turned out that two different schemes gave different width of the spectral interval of the reflected radiation (Fig.3). The difference is explained by peculiarity of usage of the directional coupler for the reflected power registration in the second scheme. This directional coupler has been designed for the wave H_{10} and therefore the power of H_{10}-wave transformed into the wave E_{12}, is not registered. Thus, the difference between the results of measuring testifies that the wave transformation is really exists.

The resonator consists of the reflectors with one-dimensional gratings has a narrow spectrum of natural modes with close values of quality factors. However, according to the computer simulations [3] the regime of a single-mode oscillation can be set as a result of modes competition at a non-linear stage of generation.

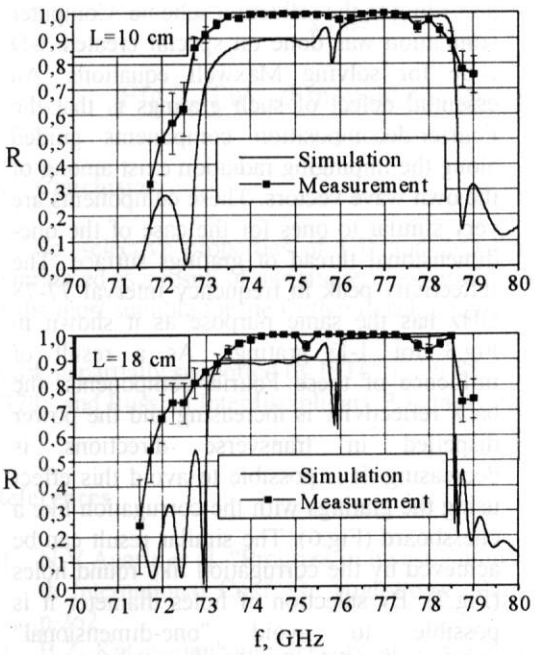

Fig.2. Reflectivities of the one-dimensional Bragg reflectors.

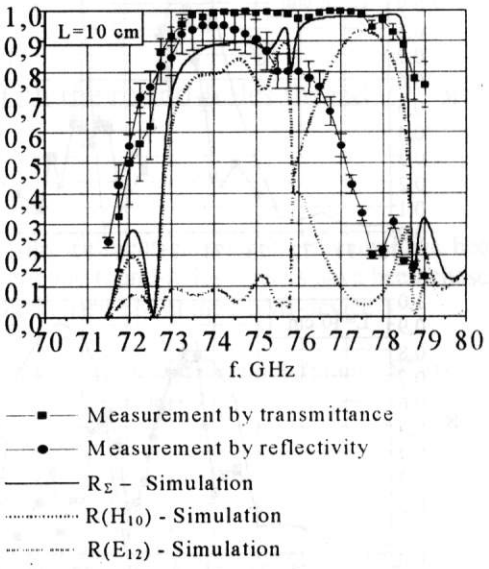

Fig.3. Comparison of measuring by different schemes.

3. 2-D reflectors.

If transverse size of a sheet beam is too much the diffraction divergence of radiation becomes insufficiently for a spatial coherence of the radiation. In this case it is necessary to use Bragg reflectors with the corrugation of the grating surface on two co-ordinates with perpendicular directions. For usage at the ELMI-device quite easily manufactured two-dimensional gratings were designed (see Fig.4). The thread of these gratings was like two sets of perpendicular strips and Fourier-decomposition for this surface has a lot of wave vectors. Spectral behaviour of the reflectivities for reflectors consisted of such gratings are represented

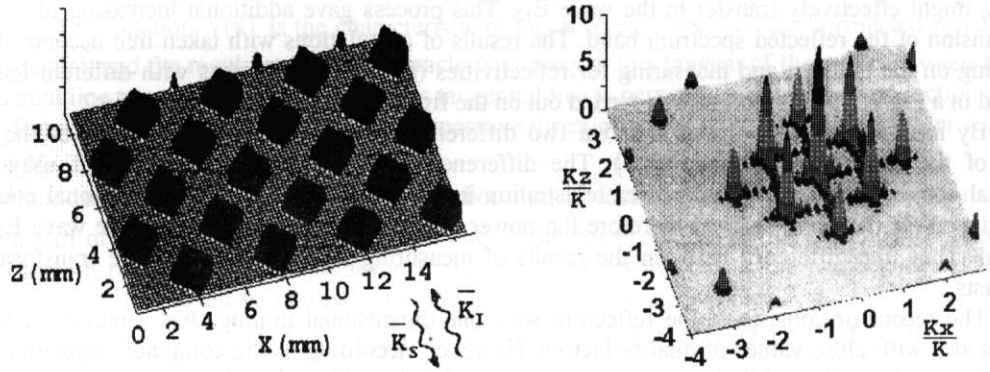

Fig.4. Two-dimensional Bragg grating with the rectangular thread.

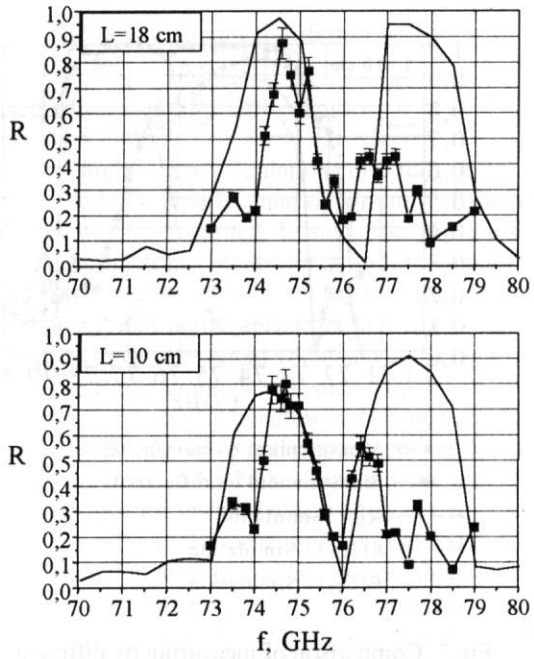

Fig.5. Reflectivities of two-dimensional Bragg reflectors.
Square points – measurement,
Solid line – simulation.

in a Fig.5. The measuring was carried out according to the reflection scheme. Computer simulation was done on special created 3-D code for solving Maxwell equations. An essential defect of such gratings is that the Fourier-decomposition components guided along the impinging radiation exist among of the own wave vectors. These components are very similar to ones for the case of the one-dimensional thread of gratings surface. The reflectivity peak in frequency interval 77-78 GHz has the same purpose as it shown in Fig.3 for 1-D gratings. As a result of influence of these Fourier-components, the back reflectivity is increasing and the power dispelled in transverse directions is decreasing. It is possible to avoid this effect using the gratings with the corrugation like a chessboard (Fig.6). The similar result can be achieved by the corrugation like round holes (Fig.7). By selection of holes diameter it is possible to avoid "one-dimensional" components of the Fourier-decomposition.

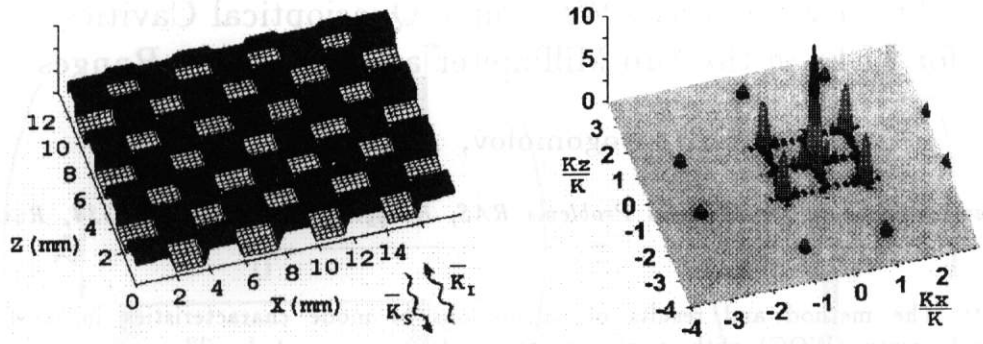

Fig.6. Two-dimensional Bragg grating with the chessboard thread.

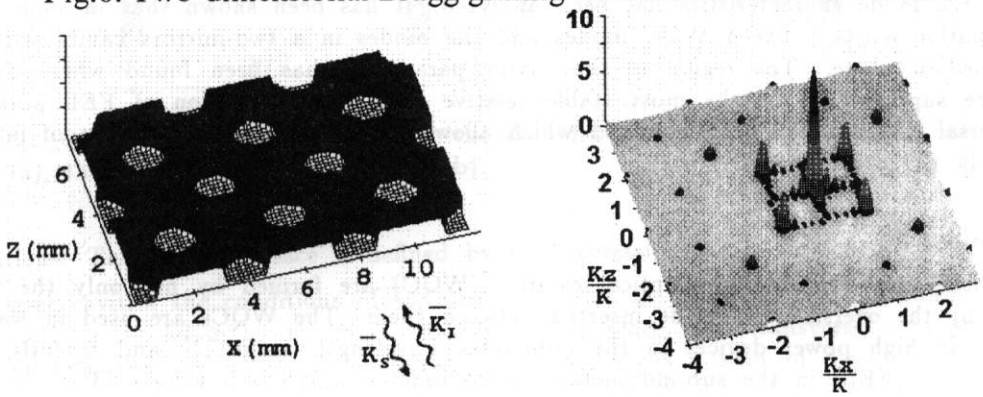

Fig.7. Two-dimensional Bragg grating with the round-holes thread.

4. Conclusion

So, selective properties of 1-D and 2-D Bragg gratings with different corrugation threads have been determined as a result of our studies. 2-D gratings with chessboard and round-holes threads have been chosen as the most suitable for the further development of the studies on planar FEM at the ELMI-device.

Work is partially supported by ISTC (grant #531), Russian Foundation for Basic Research (grant # 97-02-7379), and Russian Interdisciplinary Program "Physics of Microwaves" (project # 1.3).

References

[1] N.V.Agarin et al. "Progress in investigations on microwave FEL driven by microsecond sheet beam"12-th International Conf. On High-Power Particle Beams (Haifa, Israel, 1998). Program and Abstracts, p.262.

[2] B.Z. Katzenelenbaum. Theory of non-regular waveguides with slowly changing parameters. Moscow, 1961 (in Russian).

[3] N.S.Ginzburg et al. "To the possibility of generation on the supermodes in the Free Electron Laser with transverse-developed interaction space", ZhTF letters, 1999, t.25, n.5, p.28-34 (in Russian).

Apparatus for Investigation of KAERI FIR FEL Radiation

Vitaly V. Kubarev*, Young Uk Jeong, Byeong Cheol Lee, Sung Oh Cho, Sun Kook Kim and Jongmin Lee

**Budker Institute of Nuclear Physics, Lavrent'ev ave. 11, 630090, Novosibirsk, Russia*
Lab. For Quantum Optics, Korea Atomic Energy Research Institute, P.O. Box 105, Yusong, Taejon 305-600, Korea

Abstract: Apparatus for investigation of KAERI FIR FEL radiation and experimental results are presented.

1. Introduction

For measurement radiation of KAERI FIR FEL [1] high-sensitive infrared, sub-millimeter and millimeter detectors and mesh Fabry-Perot interferometers were developed.

2. Detectors

Liquid helium cooled Ge:Zn, Ge:Ga and In:Sb photo-resistors were used as sensitive elements of the detector in MIR, FIR, sub-millimeter and millimeter range. Detectors have noise equivalent power NEP = 10^{-11} – 10^{-10} W/Hz$^{1/2}$ and response time ~ 100 ns. Photo-resistors were placed in special chamber inside the dewar of EG&G Judson Co. which had small size and so was very convenient in work and easily screened from X-ray radiation (Fig.1). After our modernization liquid helium life time in this dewar was increased in 4 times up to 11 hours that was quite enough for one-day physical experiment. Unique property of our Ge:Ga detector is its unusual wide-range sensitivity. Measurement radiation from 20 μm to ~1 mm is possible by using only one this detector. In KAERI FIR FEL experiment it is used to detect spontaneous and laser emission with wavelengths 90–160 μm and undulator betatron radiation on wavelength ~ 1 mm.

3. Spectrometer

Fabry-Perot interferometers based on copper and nickel meshes were used as spectrometers. Different meshes and different distances between meshes were applied in various optimum interferometers. Spectrum scanning is carried out by simplest rotation of the device. Spectral resolution $(4–8)\times10^{-4}$, transmittance 70–90 % and range of free dispersion $(1–2)\times10^{-2}$ was typical parameters of the Fabry-Perot interferometer. One of the instrumental functions of the device is presented in Fig.2.

4. Calibration

Calibration of detectors, spectrometers, absorbers, windows and another equipment was carried out by using of universal RF-discharge laser [2]. This laser generates various lines of infrared and sub-millimeter range in CW mode.

5. KAERI FIR FEL Radiation

Two different types of radiation were measured in these first experiments. First of them is the main spontaneous and laser emission in range 90–160 μm (Fig.3, Fig.4). Because of coherent effect spontaneous emission had view spikes and value spontaneous power in maximum was in 300 times more than incoherent spontaneous emission (Fig.3).

The second was radiation near ~1 mm due to vertical betatron oscillation of electron beam in undulator (Fig.5). Measurement of this radiation was very useful in our experiments because minimal betatron radiation corresponded to the best alignment of electron beam. After such alignment and drawing near to real resonance length of optical resonator we could found starting of laser process (Fig.4)[1].

References

[1] Young Uk Jeong et. al. "Compact Far-Infrared Free-Electron Laser Driven by a Microtron", Proc. of AFEF'99.

[2] Kubarev V.V. Quantum Electronics **26**(3), 191 (1996).

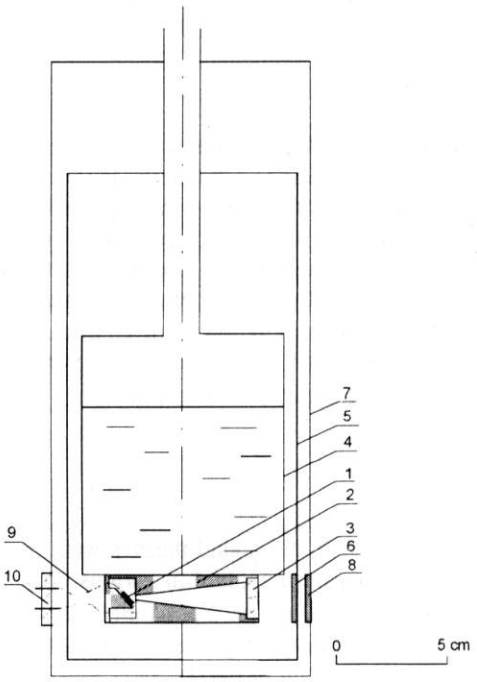

Fig.1. Schematic construction of Ge:Ga detector: 1 – photo-resistor (Ge:Ga), 2 – optical chamber, 3 – quartz cold window, 4 – liquid helium vessel, 5 – radiation shield, 6 – teflon cold window, 7 – vacuum case, 8 – teflon window, 9 – leads, 10 – electrical connector.

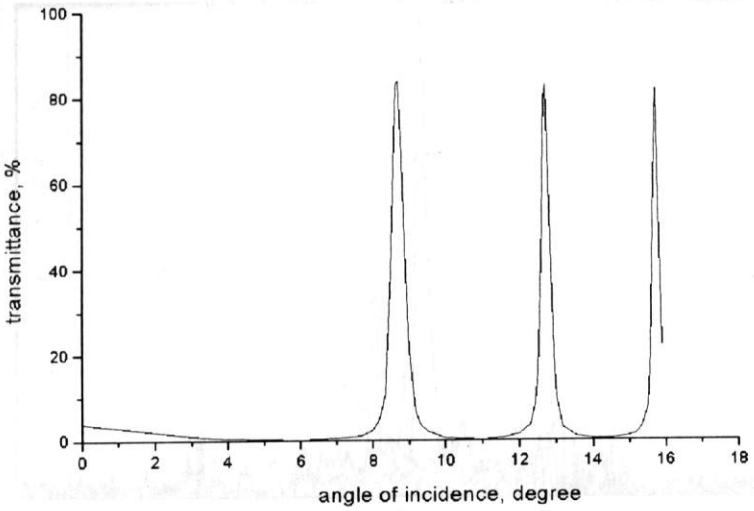

Fig.2. Typical instrumental function of the mesh Fabry-Perot interferometer measured by universal laser (28 μm line). Distance between meshs – 1.1 mm, diameter of light aperture – 42 mm, resolution – 8×10^{-4}, transmittance – 90 %, range of free dispersion – 1.3×10^{-2}.

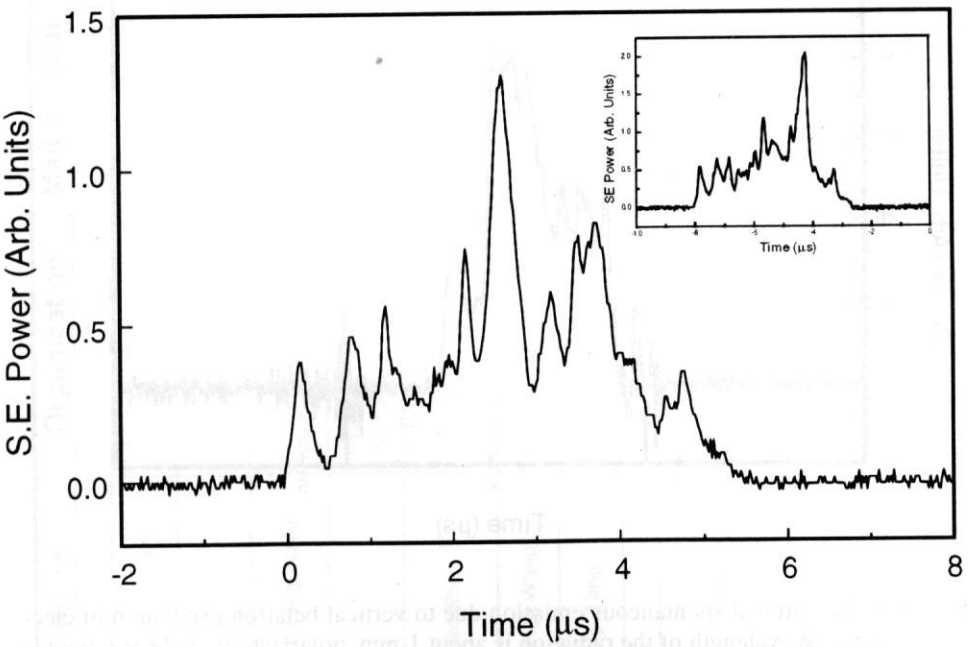

Fig.3. Signal of the main coherent spontaneous emission in wavelength 115 μm. Mirrors of optical resonator are removed.

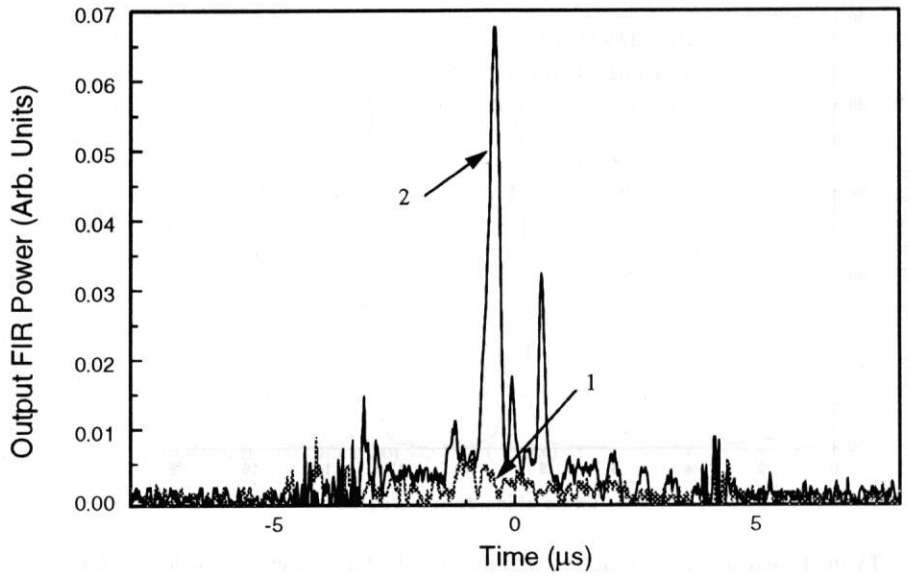

Fig.4. Signal of 115 μm radiation in resonator with mirrors: 1 – distance between mirrors is far from resonance length, 2 – distance between mirrors near to resonance length.

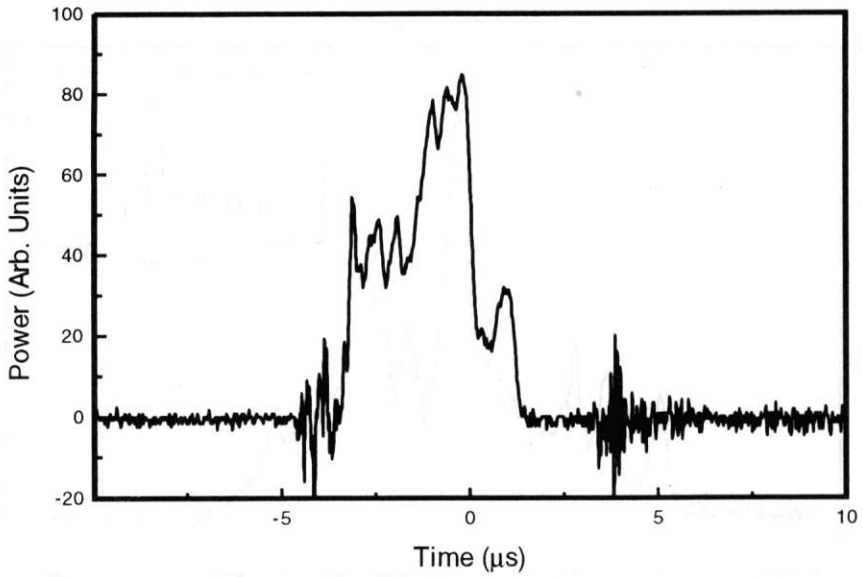

Fig. 5. Signal of additional spontaneous emission due to vertical betatron oscillation of electrons in undulator. Wavelength of the radiation is about 1 mm, polarization of electric field is vertical. Mirrors of optical resonator are removed.